

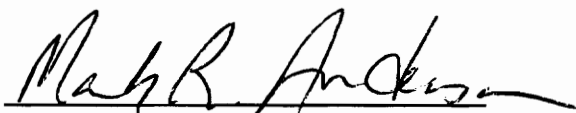
Influence of Cation Size and Surface Coverage upon the Infrared Spectrum of Carbon Monoxide Adsorbed on Platinum Electrodes

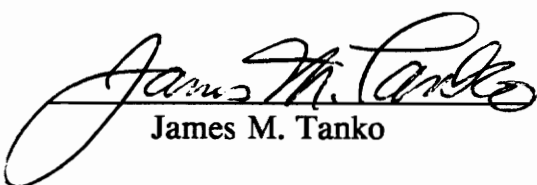
by
Jimin Huang

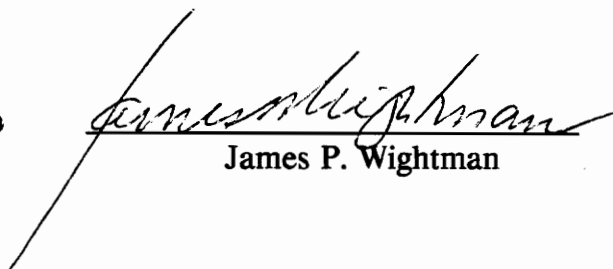
Thesis submitted to the Faculty of the
Virginia Polytechnic Institute and State University
in partial fulfillment of the requirements for the degree of

Master of Science
in
Chemistry

Approved:


Mark R. Anderson, Chairman


James M. Tanko


James P. Wightman

July, 1991
Blacksburg, Virginia

c.2

LD

5655

V855

1991

#828

C.2

Influence of Cation Size and Surface Coverage upon the Infrared Spectrum of Carbon Monoxide Adsorbed on Platinum Electrodes

by Jimin Huang

Committee Chairman: Mark R. Anderson
Chemistry

(ABSTRACT)

Adsorbed carbon monoxide is utilized as a double layer probe molecule because of its strong absorption in infrared region and because of the high sensitivity of the carbon-oxygen bond to changes in the environment local to the electrode surface. Potential Difference Infrared Spectroscopy was used to investigate the structural behavior of CO adsorbed on a platinum electrode. Carbon monoxide was found to be exclusively linear-bonded on platinum electrode in the presence of tetra-*n*-alkylammonium perchlorate/acetonitrile. No bridge-bonded species were observed. It was also found that the IR peak position of adsorbed CO is linearly dependent upon applied electrode potential, in agreement with Electrochemical Stark effect. The Stark tuning rate of adsorbed CO was determined to be inversely proportional to electrolyte cation size. This quantitative relationship between the Stark tuning rate and cation size is the first time that this has been experimentally demonstrated. Statistical treatment proved that surface coverage influences the rate of infrared peak position shift. The effect of surface coverage upon the conformation of tetra-*n*-octylammonium cation was also observed. Data suggested that tetra-*n*-octylammonium cation changes its conformation with surface coverage.

Acknowledgements

The author would like to thank Professor Mark R. Anderson for his patience, understanding, and guidance during my graduate studies. It was a wonderful experience to work in Anderson's group. I will miss the past two years that I spent at Virginia Tech and this memory will never fade from my mind for the rest of my life.

I would also like to thank Dr. Lee Kang whom helped me to get acquainted and adjust myself to a different culture and life style when I first came to America. Marilyn O'Grady, John Roush, and David Thacher, you guys create a warm atmosphere which eased this shy and conservative oriental whose home is thousands miles away on the other side of the earth.

Thanks my parents for their encouragement when I was down and wondering years ago. Without their support, I could never complete my education. If I have ever done anything good, it should be all attributed to my parents.

Table of Contents

ABSTRACT	ii
Acknowledgements	iii
Table of Contents	iv
List of Figures	vi
List of Tables	vii
Chapter 1 Introduction	1
1.1 <i>In Situ</i> Infrared Spectroelectrochemistry	1
1.2 Literature Review	3
Chapter 2 Theories and Experimental	8
2.1 CO as a Double Layer Probe Molecule	8
2.1.1 Bonding between Carbon and Platinum	10
2.1.2 Potential Dependent Peak Positions	10
2.1.3 Linear and Bridged Adsorption	12
2.2 Theoretical Predictions	13
2.2.1 Model of Electrochemical Double Layer	13
2.2.2 Electrochemical Stark Effect	14
2.2.3 Gouy-Chapman-Stern Model	17
2.3 Instrumentation	19
2.3.1 Spectroelectrochemical Cell	20
2.3.2 Potential Difference IR Spectroscopy	22
2.4 Increasing Signal to Noise Ratio	24
2.4.1 <i>p</i> , <i>s</i> -Polarized light	28
2.5 Experimental Aspects	32
2.5.1 Purifications of Chemicals	32
2.5.2 Surface Preparations	35
2.5.3 Data Manipulation	36
Chapter 3 Results and Discussion	39
3.1 Monolayer Surface Coverage	39
3.2 Cyclic Voltammetry	40
3.3 CO adsorbed on Platinum	42
3.4 Saturated versus Unsaturated Adsorption	45
3.4.1 Effect of Surface Coverage on Stark Tuning Rate	52

3.5 Effect of Cation Size	54
3.6.1 Effect of Surface Coverage on TOAP cation	62
Chapter 4 Summary	65
References	67
Vita	70

List of Figures

Figure 2.1 Bonding between Carbon and Platinum	11
Figure 2.2 Model of Electrochemical Double Layer	15
Figure 2.3 Spectroelectrochemical Cell	21
Figure 2.4 Retroreflector and Light Path in Thin Layer	23
Figure 2.5 Single Beam Spectrum of Adsorbed CO at 0V vs. SCE	25
Figure 2.6 Single Beam Spectrum of Adsorbed CO at -0.6V vs. SCE	26
Figure 2.7 Potential Difference Infrared Spectrum of Adsorbed CO	27
Figure 2.8 <i>p</i> , <i>s</i> -Polarized Light	29
Figure 2.9 Phase Shift with Respect to Angle of Incidence	31
Figure 2.10 Instrument Diagram	33
Figure 3.1 Cyclic Voltammogram of Adsorbed CO in Aqueous Solution	41
Figure 3.2 Spectra of CO Adsorbed on Pt in Tetra- <i>n</i> -alkylammonium Perchlorate/Acetonitrile	43
Figure 3.3 Representative Spectra of CO Adsorbed on Pt in TBAP/Acetonitrile	44
Figure 3.4 Plot of Peak Position versus Electrode Potential in the Presence of 0.1M TEAP in Acetonitrile	46
Figure 3.5 Plot of Peak Position versus Electrode Potential in the Presence of 0.1M TBAP in Acetonitrile	47
Figure 3.6 Plot of Peak Position versus Electrode Potential in the Presence of 0.1M THAP in Acetonitrile	48
Figure 3.7 Plot of Peak Position versus Electrode Potential in the Presence of 0.1M TOAP in Acetonitrile	49

Figure 3.8 Effect of Cation Size upon Stark Tuning Rate 60

List of Tables

Table 2.1 Experimental Equipment and Chemicals	34
Table 2.2 Experimental Procedures	38
Table 3.1 Experiment Determined Stark Tuning Rates	50
Table 3.2 Cation Sizes	56
Table 3.3 IHP and OHP Positions	61

Chapter 1

Introduction

1.1 *In Situ* Infrared Spectroelectrochemistry

For many years, chemists have been aware of the importance of the relationship between electrode reactions and the surface of electrodes on which these reactions occur. Many attempts have been made to reveal the relationship between the electrode surface properties and electrochemical reactions. Unfortunately, strictly electrochemical measurements do not allow discrimination between the bulk behavior of an electrochemical system and the surface behavior. It is very difficult to focus on species adsorbed on the surface of electrodes electrochemically. Historically, chemists correlated electrochemical data with surface properties by means of mathematical modeling. No direct first-hand structural data at the electrode-solution interface could be obtained to support those mathematical models until the recent development of *in situ* vibrational spectroelectrochemistry.

In situ infrared spectroelectrochemistry [1-3] is a combination of infrared spectroscopy and electrochemistry measurements. That is to say, this technique allows two measurements simultaneously. With such techniques, one can obtain both macroscopic information from electrochemical data and complementarily microscopic structural information from infrared spectra. It has been shown in the past few years that this technique is a powerful tool in surface analysis. Applications in

electrochemistry include the study of the surface structures, bonding, interaction and dynamics of adsorbates and the effect of electric field on these parameters, the monitoring in various solvent-electrolyte systems of the potential dependent concentrations for molecular and ionic species in the adsorbed state and in the electrical double layer, and the identification and reactions of adsorbed and nonadsorbed electrochemical reaction intermediates such as organic ion radicals. Perhaps the most important advantage is that *in situ* infrared spectroelectrochemistry may provide information about bonding and orientation of adsorbates on the surface of electrodes. The technique has opened an opportunity for studying the properties of the electrochemical double layer and solution-electrode interface which were not possible with strictly electrochemical measurements. Detailed interfacial information is no longer an unsolved problem in electrochemistry since the advent of surface reflection spectroelectrochemistry.

In addition, by carefully choosing adsorbates and experimental conditions, the roles of solvents and supporting electrolytes in an electrochemical process can be well understood, allowing one draw a detailed picture of the electrochemical double layer structure and the solution-electrode interface. Such information may benefit chemists in designing chemically modified electrodes, understanding the chemistry of interferences on electrodes, and utilizing electrocatalytical reactions.

1.2 Literature Review

The first surface reflection vibrational spectroscopy was demonstrated by Fleischmann et al. [4] in 1973 at the University of Southampton, Southampton, England. This measurement was an *in situ* Raman spectrum of mercurous chloride, mercurous bromide, and mercuric oxide adsorbed on a mercury/platinum substrates. This measurement started the development of surface-enhanced Raman Spectroscopy (SERS). SERS needs a rough reflection surface to observe the effect. Electrochemistry, however, prefers a smooth electrode surface. This conflict promoted the development of *in situ* infrared spectroscopy which has been extensively using in electrode surface analysis.

The application of infrared spectroscopy to the study of electrochemical systems was subsequently shown by Bewick et al. using external reflectance technique in 1979 [5,6]. Since then, rapid growth in the field of *in situ* infrared spectroscopy initiated a new age for electrochemical surface study, and became one of the major techniques utilized to investigate species adsorbed on electrode surface.

Russell et al. reported the measurement of infrared spectrum of carbon monoxide adsorbed on the surface of a platinum electrode in the presence of 1M sulfuric acid or perchloric acid as the supporting electrolyte [7]. The band of carbon monoxide stretching vibration was found to shift with applied electrode potential. Moreover, the shift of IR band illustrated a coverage dependent property.

A widely cited theoretical treatment of CO adsorbed on electrode surfaces

for in situ spectroelectrochemistry was published by Lambert [8 - 11]. He introduced the theory of vibrational Stark effect on adsorbed species for electrochemical systems and deduced a relationship between the frequency shifts of the adsorbate and the local electric field at electrode surface. From this theory, the estimated rate of frequency shift for carbon monoxide adsorbed on a platinum electrode was reported as $30 \text{ cm}^{-1}/\text{V}$, based on the Stark tuning rate of carbon monoxide adsorbed on Ni. This value is in good agreement with experiments.

Kunimatsu et al. studied the carbon monoxide adsorbed on a smooth platinum electrode in the presence of 1M perchloric acid, sulfuric acid, and hydrochloric acid aqueous solutions [12]. They found that the infrared spectra of the CO shifted with applied electric field. The rate of shift was found to be about $30 \text{ cm}^{-1}/\text{V}$, in agreement with Lambert's calculations. The shift was independent of the identity of the acidic electrolytes. It was also observed that the peak position shifted linearly even when the coverage of CO decreases appreciably and CO starts to oxidize.

Beden et al. found the effect of surface coverage upon the bonding of carbon monoxide on electrode in the presence of aqueous solutions and crystalline structure of the metal substrate [13 - 15]. Crystalline structure also changed the content and nature of the surface carbon monoxide. The quantities of linearly and bridged-bonded carbon monoxide are dependent upon the surface coverage on a polycrystalline Pt electrode. Both infrared reflectance spectroscopy and electrochemical voltammetry showed that linearly bonded carbon monoxide is

generally the major adsorbed species on all single crystal surfaces [16]. However, it became surface coverage independent when the electrode is single crystalline Pt (100).

M. R. Anderson et al. determined the Stark tuning rates for carbon monoxide adsorbed in the presence of several organic solvents and binary mixtures of the organic solvents and water [17, 18]. In these binary solvents, it was found that the Stark tuning rate changed dramatically with the percentage of water in the bulk mixture. The potential dependent peak positions were linearly dependent upon the electric field over the range investigated except for methanol solutions where three distinct different linear regions were observed. This observation was attributed to traversing the potential zero charge of the electrode. The carbon monoxide adsorption in these reports were obtained by an oxidative decomposition of a carbonyl metal complex. It was later reported by Love and McQuillan that the CO infrared peak position was linearly dependent upon applied electrode potential in double layer region and did not demonstrate the three regions reported by Anderson et al. [19]. Here the surface preparation was obtained from a methanol solution saturated with carbon monoxide. The difference in the surface preparations may account for the different observations.

Ashley et al. reported a cation effect on vibrational frequencies of adsorbed thiocyanate on platinum. The effect of four alkali metal cations, Na^+ , K^+ , Cs^+ , and Li^+ , was observed and differences were attributed to the changes of distance from

outer Helmholtz plane (OHP) to the surface of the electrode for the different cations [20]. However, data only showed the nature of the dependence of Stark tuning rate (except lithium ion); no quantitative relationship between cation size and Stark tuning rate was determined.

Alfred B. Anderson used the atom superposition and electron delocalization molecular orbital (ASED-MO) theory to calculate properties and behavior of adsorbate molecules as functions of band shift, and interpreted the calculated results by perturbation theory [21,22]. His calculations predicted that bridged adsorption (the carbon of CO is bonded with two platinum sites) of carbon monoxide on electrode surface can be stabilized by applying a negative potential of about -0.2V to the electrode. Although electrochemical data of such low negative potential have not yet been found to support this predication. Ultra high vacuum experiments conducted by Garfunkel et al. showed an increase in site conversion at negative electrode potential with increasing coverage of potassium coadsorption on platinum surface [23].

Weaver et al. also physically adsorbed carbon monoxide from a saturated solution onto the Pt electrode in the presence of THF, acetonitrile, and methylene chloride containing tetra-*n*-butylammonium perchlorate (TBAP) and sodium perchlorate as supporting electrolyte [24]. Their peak position versus applied potential data were not linear at the potential extreme. This may be due to the desorption of carbon monoxide at extreme potentials. Observation of bridged-

bonded carbon monoxide at negative potentials was found in the presence of 0.15M sodium perchlorate/acetonitrile solution. This supports the theoretical prediction of Anderson et al..

1.3 Research Objectives

The objectives of this research were (i) eliminate the interferences from surface preparation in order to have a pure and clean system to study the surface behavior of adsorbed carbon monoxide, (ii) use acetonitrile as the solvent to provide a wider applicable potential window to the system for studying the behavior of CO, (iii) study the effect of cation size upon IR spectrum of adsorbed carbon monoxide, (iv) investigate the influence of surface coverage upon the spectra of adsorbed carbon monoxide, and (v) verify theoretical predictions with experimental data.

Chapter 2

Theories and Experimental

2.1 CO as a Double Layer Probe Molecule

Carbon monoxide has been extensively used historically in the study of surface adsorption. Many publications about carbon monoxide on surfaces have been reported [5 - 27]. There were many advantages for utilizing carbon monoxide as a double layer probe molecule on the surface of electrode. First, carbon monoxide is strongly adsorbed on platinum surfaces. One may adsorb a large amount of carbon monoxide onto a platinum electrode without too much difficulty. According to Beer's Law, absorption of light radiation is directly proportional to the concentration of species in the light path. This implies that the more the carbon monoxide on the surface of platinum electrode, the better the signal to noise ratio (S/N). A strong adsorbate such as carbon monoxide largely enhances instrument response for the interface because it accumulates at the surface. Another advantage of using carbon monoxide as a probe molecule is the strong interaction of monoxide with infrared radiation. Carbon monoxide in solution-electrode interface absorbed infrared radiation at a lower frequency than free CO, approximately 2080 cm^{-1} , and probably its infrared absorption is among the strongest of all functional groups. Even though carbon monoxide is strongly adsorbed, but there is limited surface area on the electrode for the adsorption, hence, the surface concentration of carbon

monoxide is much lower than any species in solution. The surface concentration of carbon monoxide adsorbed for an aqueous solution was found to be 1.85×10^{-9} M/cm², in agreement with literature values [25 - 27]. Such a low surface concentration is very difficult to detect by infrared spectroscopy if the adsorbate interact weakly with infrared radiation. Fortunately, this weakness was partially relieved by the increase in S/N due to the strong infrared absorption of carbon monoxide. Furthermore, the degree of bonding (bond order) between the carbon of carbon monoxide and platinum is highly sensitive to changes in electrode potential. As the bond order of carbon-platinum is changed with respect to applied electrode potential, the stretching frequency changed in such a manner to reflect the variation of bond strength, allowing easy detection by infrared spectroscopy. As a matter of fact, the peak frequency of carbon monoxide is a function of applied electrode potential. In addition to the peak position shifts with changing electric field, there are two types of bonding between carbon and platinum, i.e. linear and bridged bonding, which give rise to the possibility to observe the conversion from linear to bridged adsorption under the influence of applied electrode potential as predicted theoretically by Anderson. All the factors mentioned above have made carbon monoxide and its isoelectric analogues popular for study in spectroelectrochemical studies.

2.1.1 Bonding between Carbon and Platinum

The bond between the carbon of carbon monoxide and the platinum substrate comes from the σ donation of lone-pair electrons from a carbon monoxide orbital to an empty platinum orbital (Figure 2.1) [28]. The electrons from a filled platinum d orbital may be interact with the empty CO π^* orbital which results a π back donation. By altering the electrode potential we may change the donating and withdrawing ability of surface. This in term may alter the vibrational frequency of the adsorbed carbon monoxide.

2.1.2 Potential Dependent Peak Positions

A change in potential to more positive value deposits more positive charges on electrode surface and increases the strength of electric field above electrode. It induces a stronger attraction to withdraw the lone-pair electrons of CO toward platinum and hence strengthens the σ platinum-carbon bonding. It also withdraws the electron cloud of d orbital back to platinum that the π back bonding is weakened. Therefore, the CO π bond is strengthened so that its vibrational frequency increases. On the other hand, as the electrode potential becomes more negative, the electromagnetic force from the electrode pushes the back donation of platinum d electrons more into CO π^* orbital. The extent of overlap between platinum d orbital and CO π^* orbital is thus increased. This increasing in antibonding weakens the CO bond which vibrates at lower frequency.

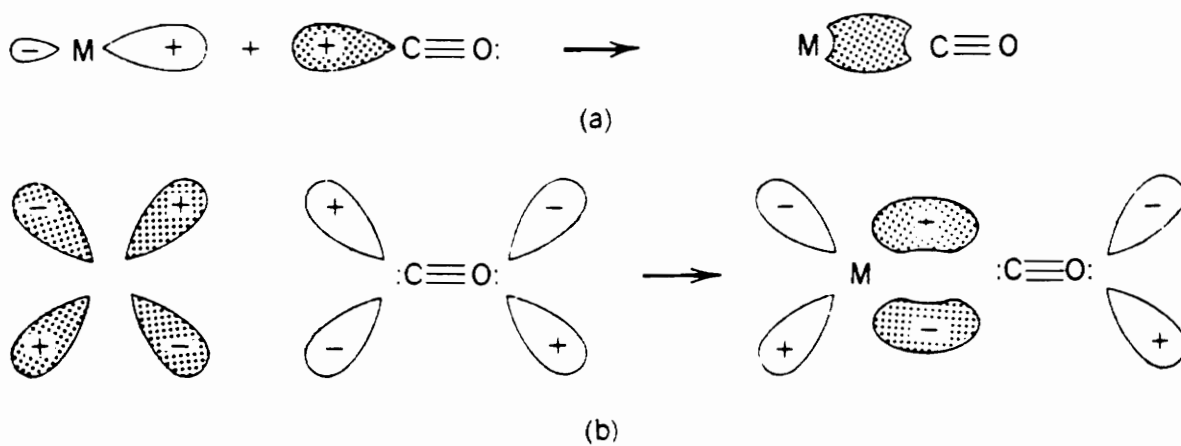


Figure 2.1 Bonding between Carbon and Platinum. (a) σ Donation from carbon to platinum. (b) Back Donation from metal into CO orbital.

2.1.3 Linear and Bridged Adsorption

The σ and π back donations make a single bond between carbon and platinum which is called linear adsorption. This electron arrangement arises another way to distribute electrons in order to relieve the high electron density between carbon and oxygen. Since the carbon of CO possesses a -1 formal charge and there is a triple bond between carbon and oxygen, as a result, the oxygen of CO carries a +1 formal charge [29]. A conversion from linear to bridged adsorption can solve the charge separation problem on carbon monoxide. The so called "bridged adsorption" has a decreased bond order between carbon and oxygen, that is to say, the formal charges on carbon and oxygen are both neutral and the carbon of CO is bounded with two platinum sites. It acts like a bridge between two platinum sites. Infrared peak frequency of bridged adsorption occurs at about 1750 cm^{-1} , behaving quite similar to an organic carbonyl group (approximately 1720 cm^{-1}). Almost all carbon monoxide molecules are linearly adsorbed on platinum naturally. Bridged adsorption is rarely found when the surface is prepared by traditional methods. However, Anderson et al. [21, 22] suggested in their molecular orbital calculations that carbon monoxide prefers bridged to linear bonding on electrode at extreme negative potentials. That was because negative potential increases the extent of π back donation, destabilizing CO π bond and thus increasing the stability of bridged bonding. A shift in potential to extreme negative potential might give an opportunity to convert carbon monoxide from a linear bonding to the bridged bonding. Weaver's report [24] of site

conversion in the presence of sodium perchlorate as the supporting electrolyte in acetonitrile correlated with Anderson's calculations. One thing interesting in Weaver's data was that sodium perchlorate/acetonitrile was the only solvent/electrolyte combination which demonstrated this site conversion among four different electrolyte/solvent combinations tested. It might indicate that an extreme negative potential is not the only required experimental condition for a site conversion.

2.2 Theoretical Predictions

Many theories have been introduced to give a representation of the electrochemical double layer structure and the influence of electric field on carbon monoxide adsorbed on electrode surface. Many experiments have also been conducted to seek evidence to support these theories. Some of the theories of importance to this thesis are Electrochemical Stark effect, and the Gouy-Chapman-Stern model of the electrochemical double layer.

2.2.1 Model of Electrochemical Double Layer

The concept of double layer is a variance of electronic parallel-plate capacitor. Adjacent to the electrode surface, there are adsorbed solvent molecules and other adsorbed species to form a contact adsorbed layer. This layer is called "Inner Helmholtz Plane" (IHP). Adjacent to IHP, solvated cations form the next

layer, called "Outer Helmholtz Plane" (OHP) (Figure 2.2) [30]. The metal surface and the OHP act like the two parallel plates of a capacitor.

According to fundamental physics, the capacitance C between two parallel plates is given by [31]:

$$C = \frac{\epsilon A}{4\pi d} \quad (2.1)$$

where ϵ is the dielectric constant of the medium, A is the plate surface area, and d is the distance between the two plates.

For a given potential difference applied to the two plates, an electric field is established between the plates. One can change the electric field strength by altering the distance between the two plates. The same principle is applicable to the electrochemical double layer by changing cation size, hence the position of the Outer Helmholtz Plane. As the cation size increases, the OHP is pushed away from electrode surface. The electric field in double layer is, therefore, decreased. Because, as predicted by the Electrochemical Stark effect, the carbon monoxide peak frequency changes with the electric field in double layer, the rate of peak shift should be smaller when a cation of longer size is used as the supporting electrolyte.

2.2.2 Electrochemical Stark Effect

Lambert [8 - 11] derived the Stark tuning rate, δ , for adsorbate vibrational frequency ν with electric field E as:

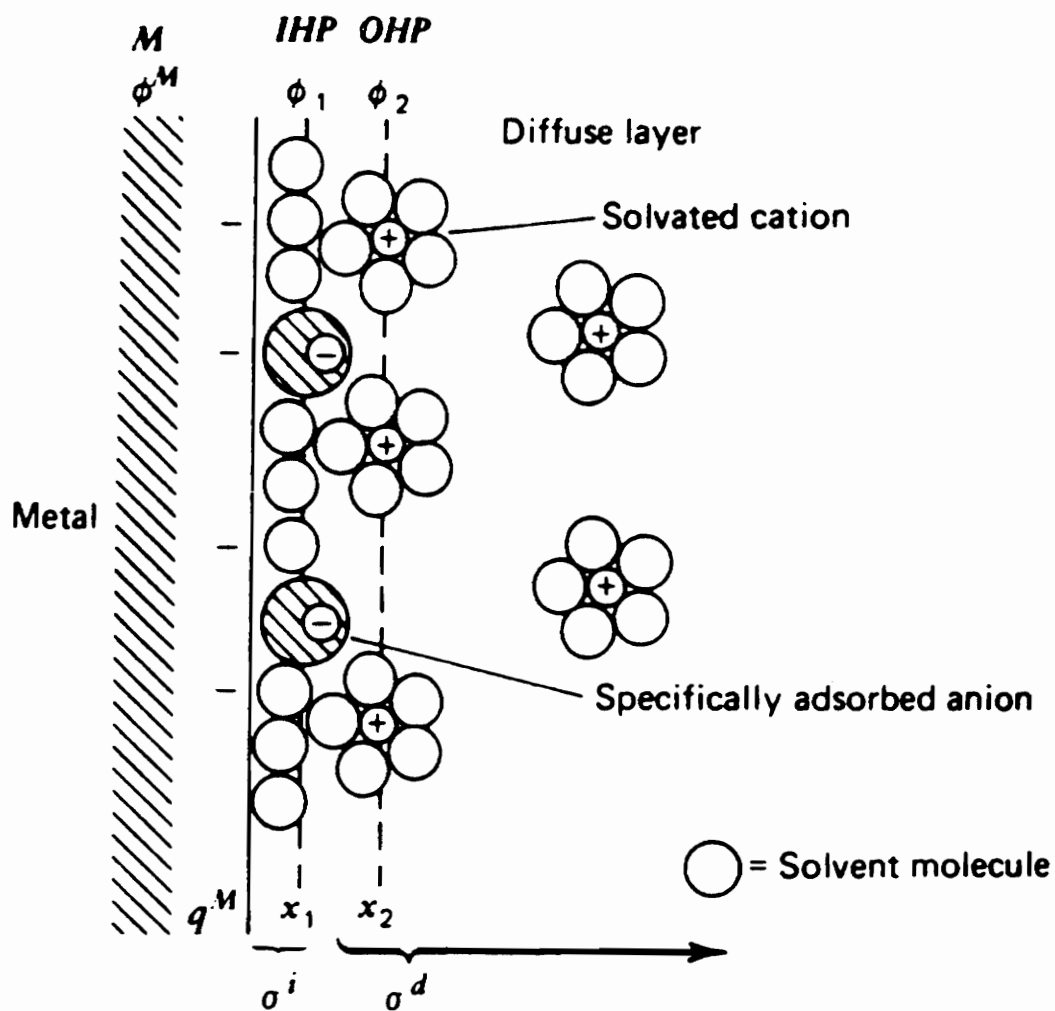


Figure 2.2 Model of Electrochemical Double Layer

$$\delta_{\nu E} = \frac{d\nu}{dE} \quad (2.2)$$

The shift of peak frequency ν with applied electrode potential V is:

$$\delta_{\nu V} = \frac{d\nu}{dV} \quad (2.3)$$

There is a linear relationship between applied potential V and electric field E , expressed by:

$$\frac{dE}{dV} = \frac{C}{\epsilon} \quad (2.4)$$

where C is the electrolyte-metal interfacial capacitance, ϵ is the dielectric constant in double layer. Applying simple chain rule to Equation 2.4 gives:

$$\frac{dE}{d\nu} \frac{d\nu}{dV} = \frac{C}{\epsilon} \quad (2.5)$$

Rearranging Equation 2.5 results:

$$\frac{d\nu}{dV} = \frac{d\nu}{dE} \frac{C}{\epsilon} \quad (2.6)$$

Substituting Equations 2.2 and 2.3 into 2.4 gives:

$$\delta_{\nu V} = \delta_{\nu E} \frac{C}{\epsilon} \quad (2.7)$$

In simple terms, electrochemical Stark effect predicts that at constant surface

concentration the rate of peak shift with applied electrode potential is linear for the whole double layer region (double layer region is a potential window where no faradaic current occurs). That is, a plot of peak position versus electrode potential should be a straight line. By carefully controlling the experiment conditions, e.g. maintaining $d\nu/dE$ as a constant, the rate of peak shift with applied electrode potential $d\nu/dV$ is a constant according to Equation 2.7 and can be measured.

2.2.3 Gouy-Chapman-Stern Model

Gouy and Chapman proposed a model of double layer structure to include some factors which were not counted in the simple capacitance model of double layer [32]. This model was then modified by Stern to give the final Gouy-Chapman-Stern model (GCS model). It states that the equivalent circuit of the differential capacitance of the double layer equals the capacitance held at the outer Helmholtz plane (OHP) in series with the capacitance of the diffuse charge. The resulting capacitance of two capacitors in serial is:

$$\frac{1}{C_d} = \frac{1}{C_H} + \frac{1}{C_D} \quad (2.8)$$

$$= \frac{\epsilon_2}{\epsilon\epsilon_0} + \frac{1}{(2\epsilon\epsilon_0 Z^2 e^2 n^0 / kT)^{1/2} \cosh(Ze\phi_2 / 2kT)} \quad (2.9)$$

where

C_d	differential capacitance of the double layer
C_H	capacitance held at outer Helmholtz plane
C_D	capacitance of the diffuse charge
e	quantity of charge on the electron
k	Boltzman constant
n^0	number concentration of each ion in a $Z : Z$ electrolyte
Z	charge magnitude of each ion in a $Z : Z$ electrolyte
T	absolute temperature
ϵ	dielectric constant
ϵ_0	permittivity of free space
ϕ_2	potential at the OHP with respect to bulk solution
x_2	distance from electrode to outer Helmholtz plane

Extracting the items in Equations 2.8 and 2.9 for the capacitance which was held at outer Helmholtz plane gives:

$$C_H = \frac{\epsilon\epsilon_0}{x_2} \quad (2.10)$$

Equation 2.10 shows the capacitance held at the outer Helmholtz plane is inversely proportional to the distance from electrode to outer Helmholtz plane. Comparing with parallel-plate capacitor, it can be found that they are very similar. That is, the capacitance C_H is determined by the position of outer Helmholtz plane above the electrode; in other words, cation size has an impact on outer Helmholtz

plane position and electric field strength. The electric field is stronger with a smaller cation as the supporting electrolyte and the rate of peak shift should be lower with bigger cations. Asheley et al. [20] successfully demonstrated this effect with the infrared peak of thiocyanide adsorbed on electrode is dependent upon the size of electrolyte cation.

2.3 Instrumentation

Instrumentation is always a challenge for surface reflection spectroscopy. There were two major problems in *in situ* spectroelectrochemistry that need to be overcome. First of all, bulk solvent absorbs most of infrared radiation and overwhelms the weak signal from adsorbates. Carbon dioxide and moisture in surrounding air also interfere with the identification of adsorption. Adsorbates are difficult to identify in a spectrum without removing those interferences. Secondly, adsorbates have an average surface concentration on the order of 10^{-9} M/cm². Compared with concentrations of species in solution, this is an extremely low concentration for infrared spectroscopy, and is very close to the limit of detection for the instrument. Eliminating interfering peaks in spectra and enhancing signal to noise ratio (S/N) were the two most important objectives in instrumentation. Many techniques from various scientific areas were adapted to facilitate these problems.

2.3.1 Spectroelectrochemical Cell

Bulk solvent absorption of infrared radiation may dominate the whole spectrum. Reducing the length of light path was a direct way which would greatly reduce the size of solvent peaks. A special spectroelectrochemical cell designed by Pons [1 - 3] fulfilled the experimental requirements. Figure 2.3 [33] shows the spectroelectrochemical cell and the working electrode used in this research. The cell and working electrode were from a modified glass syringe. At the front of the cell was a calcium fluoride optical window. Calcium fluoride is infrared transparent (cut off at 1200 cm^{-1}) and water insoluble, unlike potassium bromide and sodium chloride which are widely used as infrared windows in both organic and inorganic structure determination but forbidden for aqueous systems.

A piece of polycrystalline platinum disk was sealed on the top of syringe plunger. This platinum disk has two functions. Electrochemically, it is the working electrode which carries current and potential. Spectroscopically, it is an optical reflection mirror for the spectrometer. By assembling the plunger electrode and barrel cell a spectroelectrochemical cell was ready to have carbon monoxide adsorbed on the platinum-disk electrode/mirror. Once carbon monoxide was accumulated on the electrode to a certain amount, the working electrode was manually pushed toward the calcium fluoride optical window until it contacted with the window. Although it seemed that all the solvent has been expelled out of the light path, a thin layer of solution with a thickness estimated to be 10 - 100 microns

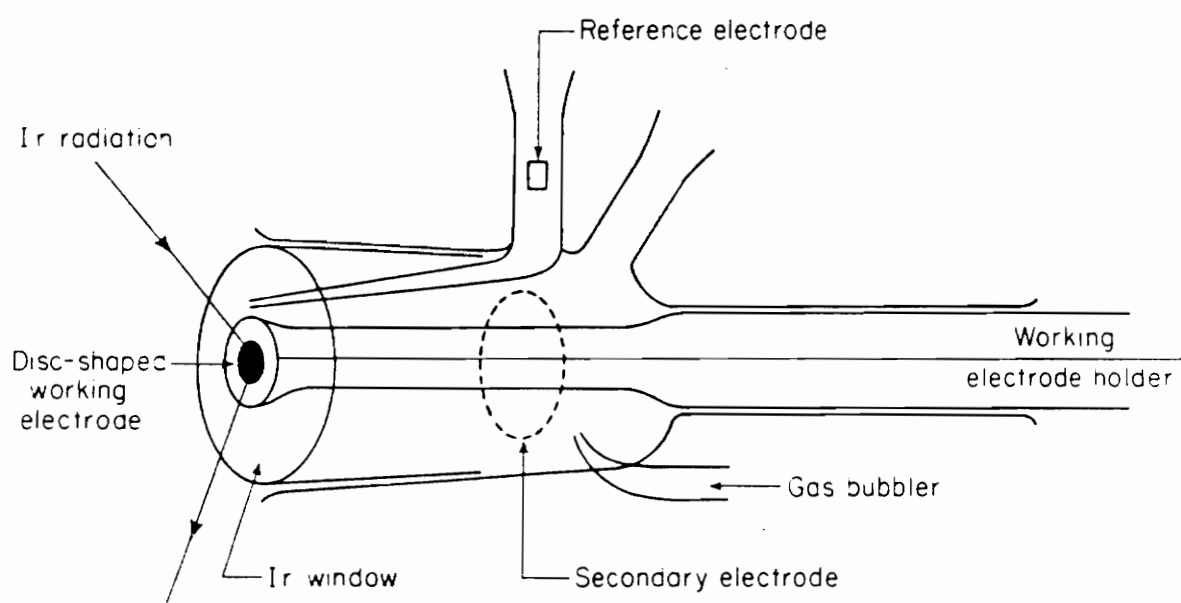


Figure 2.3 Spectroelectrochemical Cell

was sandwiched between the optical window and the platinum-disk electrode. Infrared radiation could travel through the window, the thin solution layer, and then be reflected out of the cell (Figure 2.4) [34] with minimal solvent absorption. Infrared radiation was directed onto the working electrode by means of two focusing mirrors and two reflection mirrors. The mirror-cell combination was called "retroreflector" (Figure 2.4). Infrared radiation from the source was projected into the retroreflector and the output beam was fed to an infrared detector.

2.3.2 Potential Difference IR Spectroscopy

The thin-layer spectroelectrochemical cell could not eliminate all solvent absorption. Even in the thin layer, there are many more solvent molecules and electrolyte ions than adsorbate in the thin layer. Therefore, solvent absorption still dominated the spectrum taken on the spectroelectrochemical cell. A signal processing technique called Potential Difference IR Spectroscopy (PDIRS) was used to eliminate the final solvent absorption in the thin layer [24 - 27]. This technique took advantage of the potential dependent peak position of adsorbates. Figures 2.5 and 2.6 show single-beam spectra of carbon monoxide with 0.1M tetra-n-butylammonium perchlorate (TBAP) in anhydrous acetonitrile obtained at 0.0 V and -0.6 V vs. SCE respectively. Only acetonitrile absorption is observed on the spectra where the carbon monoxide peaks of interest are embedded in the larger background absorption at about 2080 - 2100 cm^{-1} . Since solvent peaks are not potential

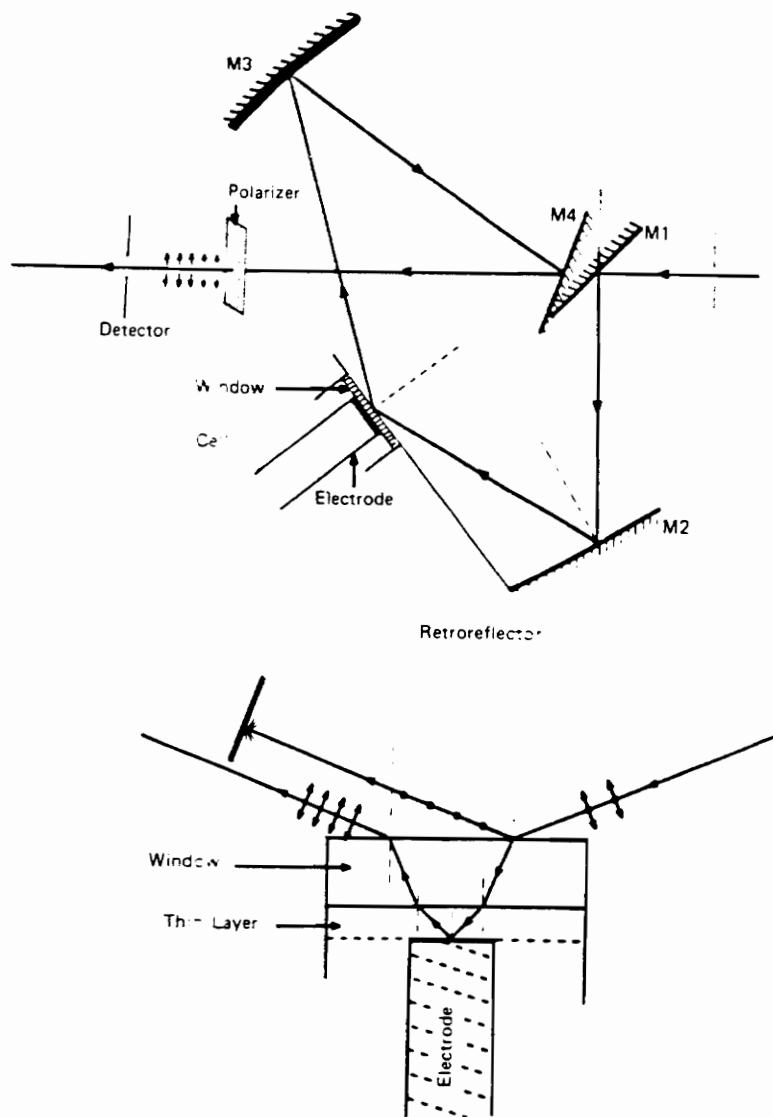


Figure 2.4 Retroreflector and Light Path in Thin Layer

dependent, only carbon monoxide peak responds to applied electrode potential. Ratioing the two spectra collected at different electrode potentials, therefore, cancels the solvent absorption. The only features left on the resulting spectrum are the potential dependent components, i.e., a positive and a negative carbon monoxide peaks (Figure 2.7). Occasionally, carbon dioxide and water moisture in surrounding air cannot be completely canceled by PDIRS because of dynamic air circulation. Carbon dioxide and water moisture can be removed by enclosing all optics and light path within purge boxes and purging with carbon dioxide and water free air at all times. All spectra in this research were collected in such fashion on a Fourier Transform Infrared Spectrometer.

2.4 Increasing Signal to Noise Ratio

Fourier transform infrared uses signal averaging to enhance its signal to noise ratio. The improvement of signal to noise ratio is proportional to $n^{1/2}$, the square root of number of interferograms accumulated. For instance, to double the signal to noise ratio one needs to quadruple the number of scans. For an enhancement of signal to noise ratio by the factor of n , the time required becomes n^2 times. However, for an unstable sample, species decay rapidly as the time elapses. Long-term scans are not allowable under such circumstance. This is the major trade-off of signal averaging by Fourier transform techniques. Therefore, one usually has to compromise between the time needed and the enhancement desired. Another

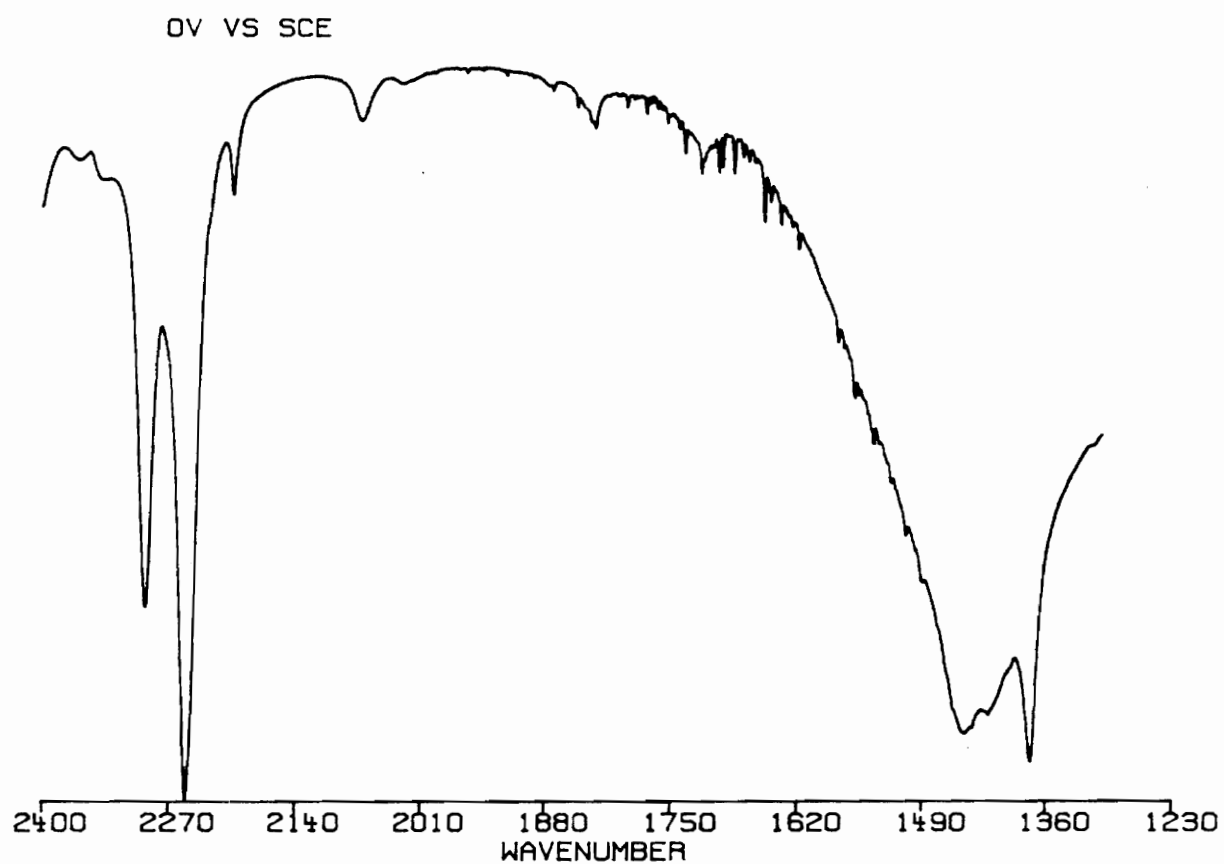


Figure 2.5 Single Beam Spectrum of Adsorbed CO at 0V vs. SCE

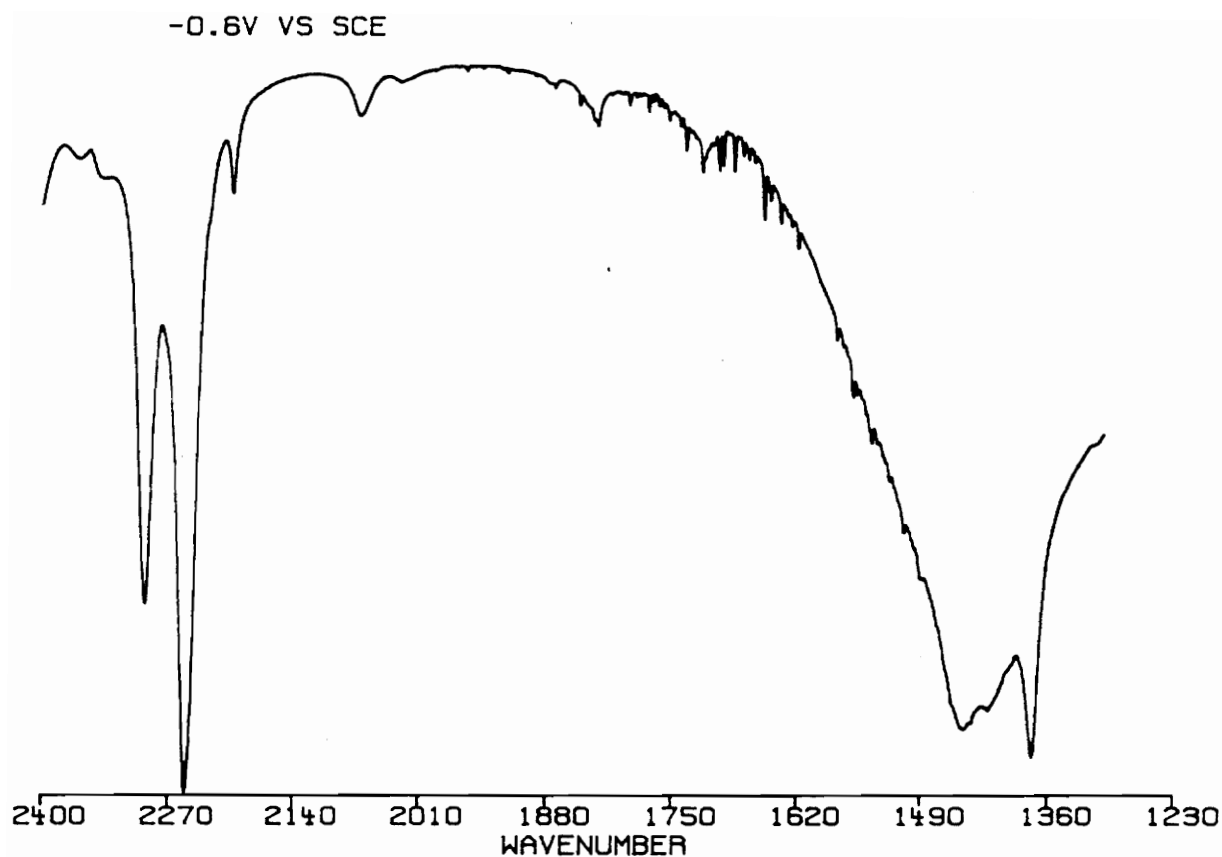


Figure 2.6 Single Beam Spectrum of Adsorbed CO at -0.6V vs. SCE

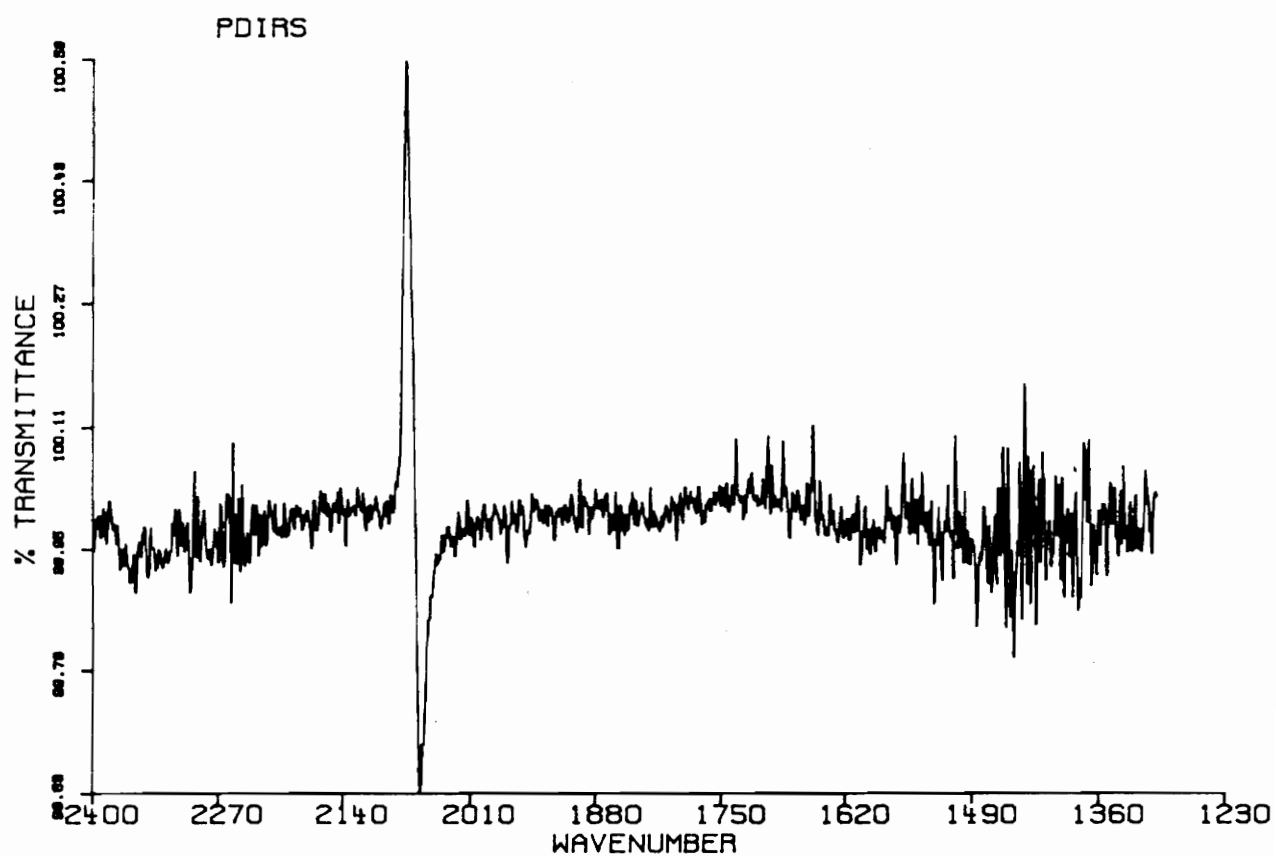


Figure 2.7 Potential Difference Infrared Spectrum of Adsorbed CO

technique was needed to give a better signal to noise ratio without sacrificing the system performance. For this reason, an infrared polarizer was placed in light path to increase the signal to noise ratio by the factor of 2 while the total data collection time is still the same.

2.4.1 *p*, *s*-Polarized light

A light wave propagated in space and reflected from a surface can be mathematically classified into two vector components (Figure 2.8) [35]. *p*-Polarized light is the component which has its electric field oscillating parallel to the plane of incidence. In other words, *p*-polarized light is the vector perpendicular to the reflection plane. *s*-Polarized light had its electric field perpendicular to the plane of incidence, that is, parallel to the reflection plane. When a beam of light incidents upon a plane surface and gets reflected, both *p* and *s*-polarized light undergo different degrees of phase shift. Calculations from Fresnel's equations [36] indicate that at all angles of incidence *s*-polarized light suffers a near 180° phase shift upon reflection from the electrode surface (Figure 2.9) [36]. The interference between the incident and reflected lights is destructive. The induced standing wave has a node on the electrode surface, i.e., there is no field intensity and hence it has no interaction with species adsorbed on the electrode surface. *p*-Polarized light, however, suffers a phase shift which is dependent on the angle of incidence. *p*-polarized light can, therefore, interact with adsorbed molecules. Summarizing the

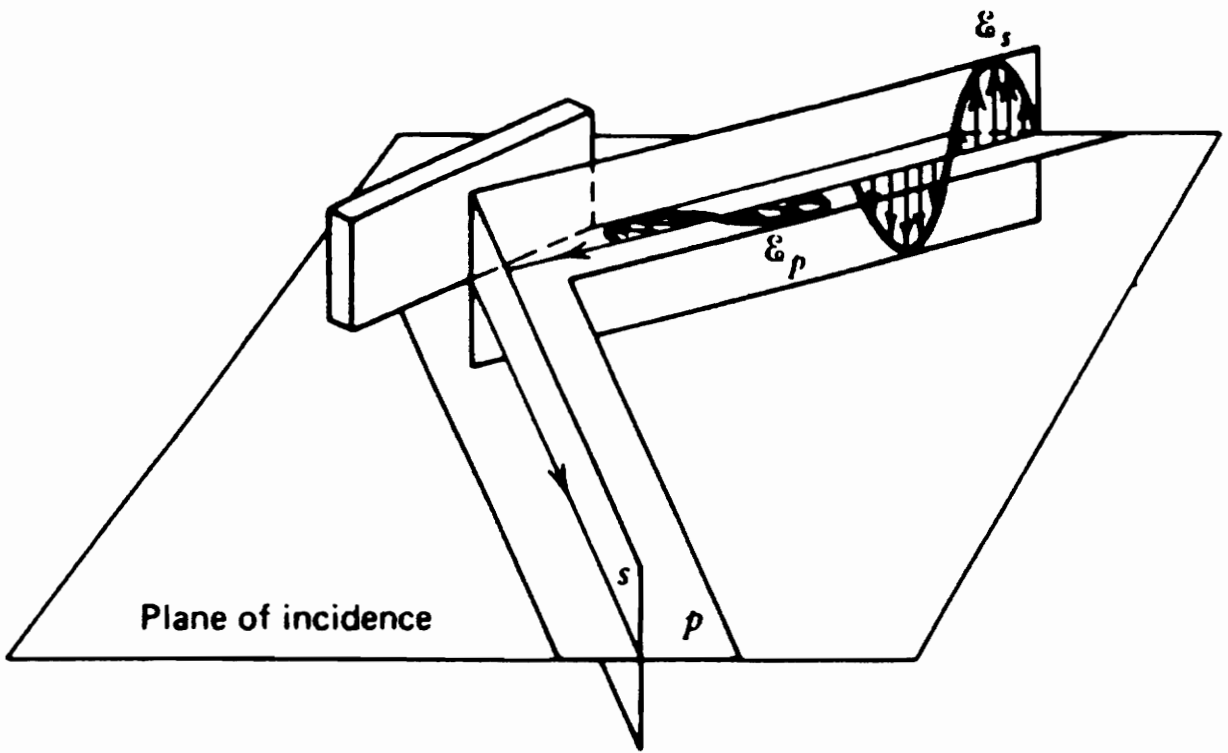


Figure 2.8 p , s -Polarized Light

effect of *p*, *s*-polarized light gives the following results:

1. *s*-Polarized light suffers a near 180° phase shift upon reflection from the electrode at all angles of incidence. The reduced standing wave has a zero intensity on electrode surface so that it can not interact with species adsorbed on electrode. Therefore, the reflected light reaching the detector contains no useful information with regard to adsorbates.
2. Both *p*, *s*-polarized light interact equally well with the species in the bulk solution such as solvents and supporting electrolyte ions which can be eliminated by PDIRS.
3. *p*-Polarized light carries all of the vibrational information about species adsorbed at the electrode surface in addition to bulk solution interaction.

In short, *s*-polarized light has no useful information for surface reflection spectroscopy. It can be removed by placing an infrared polarizer in the path of infrared beam. The removal of *s*-polarized light doubles the signal to noise ratio, because none of the signal but one half of the noise is removed by the removal of *s*-polarized light.

Figure 2.10 [37] is the complete instrument diagram. All optical mirrors, detector, and calcium fluoride window of spectroelectrochemical cell were enclosed in aluminum boxes which were purged with CO₂ and moisture free air at all times in order to reduce atmospheric interference and IR absorption of CO₂ and H₂O.

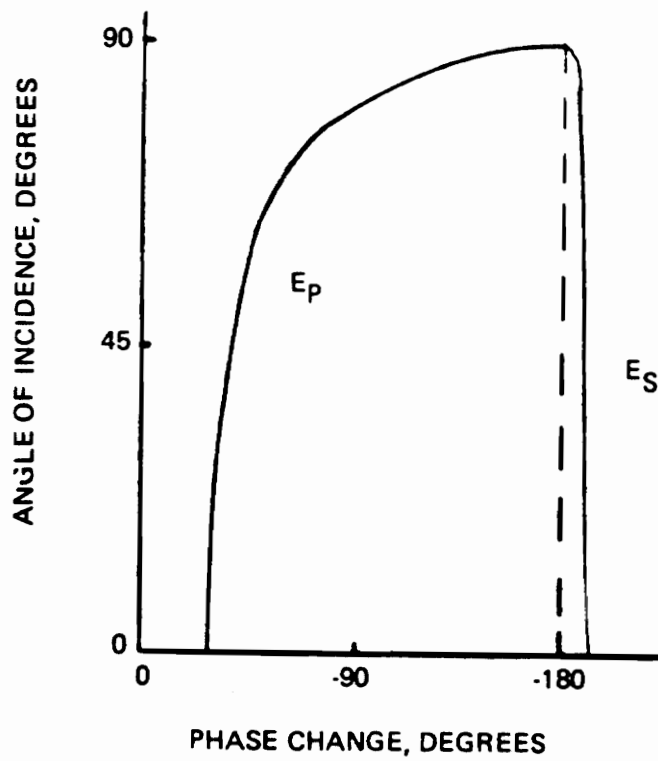


Figure 2.9 Phase Shift with Respect to Angle of Incidence. E_p represents radiation polarized parallel to the plane of incidence and E_s represents radiation polarized perpendicular to the plane of incidence.

2.5 Experimental Aspects

All experiments of this research were performed in an air-conditioned laboratory at 25°C. Table 2.1 gives the equipment and chemicals used in this research. All potentials are measured with respect to a saturated calomel electrode.

2.5.1 Purifications of Chemicals

Anhydrous acetonitrile was obtained by fresh distillation on the day of experiment from a calcium hydride treated suspension under a dry nitrogen purge. All gases were dried by a drying tube filled with anhydrous calcium sulfate as the desiccant. Because acetonitrile is a volatile liquid. Long term bubbling the solution with gases might remove part of the solvent in the spectroelectrochemical cell and increase the solution concentration. Therefore, all gases were saturated with acetonitrile vapor by an anhydrous acetonitrile bubbler before being bubbled into the spectroelectrochemical cell.

Tetraethylammonium perchlorate (TEAP) and tetra-*n*-butylammonium perchlorate (TBAP) were synthesized by the method of House [38] and recrystallized twice from water. Tetra-*n*-hexylammonium perchlorate (THAP) and tetra-*n*-octylammonium perchlorate (TOAP) were recrystallized twice from ethyl acetate/hexane solutions. All recrystallized electrolytes were dried under high vacuum for at least 24 hours and then stored in a desiccator prior to usage.

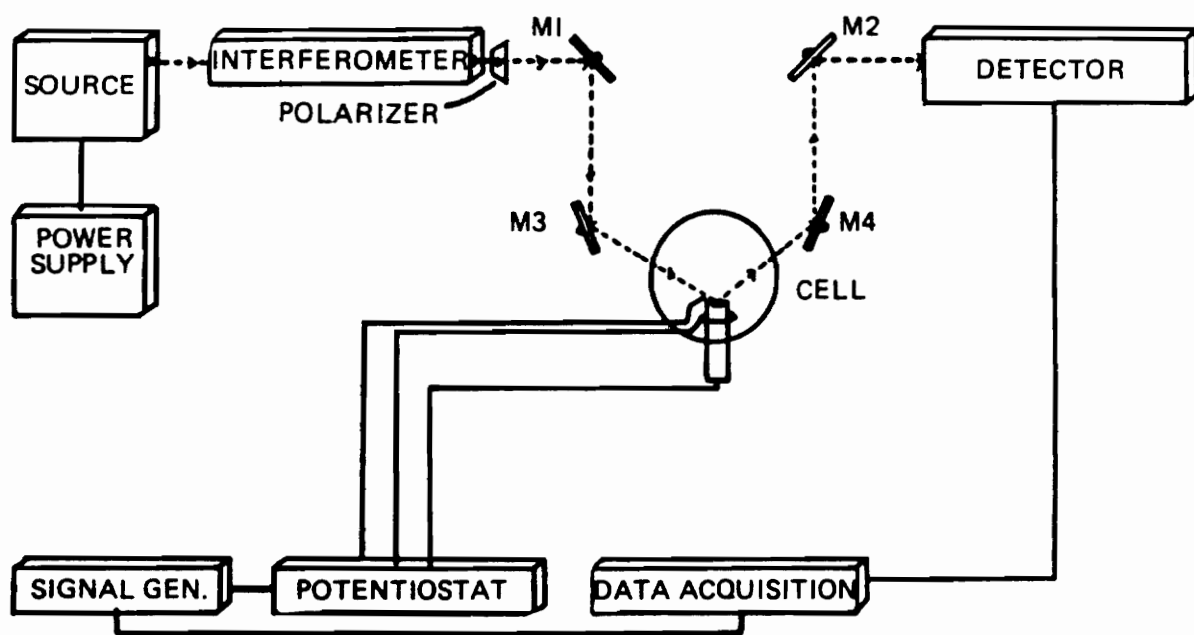


Figure 2.10 Instrument Diagram

Table 2.1 Experimental Equipment and Chemicals

Equipment

FTIR	Nicolet 710 (Nicolet Instruments, Madison, WI)
Detector	Nicolet MCT Detector (Liquid N ₂ cooled)
Potentiostat	JAS model JDP 1600 (JAS Instruments, Salt Lake City, UT)
	EG&G model 273 (EG&G Instruments, Princeton, NJ)
Air Purifier	Balston 75-60 (Balston Filter Products, Lexington, MA)
Water Purifier	Barnstead NANOpure II (Barnstead, Dubuque, IA)
Polarizer	Cambridge Physical Science
Mirrors	Nicolet, silver front surface mirrors
CaF ₂ Window	32 X 3 mm (Spectral Systems Inc., Irvington, NY)
Ref. Electrode	Saturated Calomel Electrode

Chemicals

Solvent	
Acetonitrile	Fisher Optima Grade
Ethyl Acetate	J. T. Baker
Hexane	Fisher

Electrolytes	
TEAP	Local Synthesis
TBAP	Local Synthesis
THAP	Fluka
TOAP	Fluka

Gases	
CO	AirCo
N ₂	AirCo

Misc.	
CaSO ₄	W. A. Hammond Drierite Co.
CaH ₂	Aldrich
Alumina	Buehler Micropolish (For electrode polishing)

Software

Molecular Modeling	PCModel (Serena Software, Bloomington, IN)
Linear Regression	Quatro Pro (Borland International)

2.5.2 Surface Preparations

Many methods are available to adsorb carbon monoxide onto the electrode surface. One can use either electrochemical or physical method to adsorb carbon monoxide onto the electrode. Anderson et al. [17, 18] used a redox reaction of vanadium hexacarbonyl to generate carbon monoxide. Carbon monoxide was adsorbed on the platinum surface via the oxidation and subsequent decomposition of $V(CO)_6$. Another method to obtain carbon monoxide is the oxidation of methanol at the electrode. It is not possible to oxidize methanol in acetonitrile due to the lack of oxygen source. These methods give a strong but not clean carbon monoxide adsorption due to the side products of oxidation and decomposition. Physically bubbling carbon monoxide gas into the solution contained by the spectroelectrochemical cell gives a clean carbon monoxide adsorption which is free of interferences. Excess carbon monoxide may be removed from the solution by subsequent purging with dry nitrogen.

Several ways of adsorbing carbon monoxide from the saturated solution have been introduced. One is to hold the electrode potential at a constant value while carbon monoxide is being bubbled into the solution. Another is to scan the electrode between the potential limits established by the solvent/electrolyte in the solution saturated with carbon monoxide. The former gives a poor and unstable adsorption on electrode so that it is not practical to meet the experimental requirement for surface reflection infrared spectroscopy. The latter ends with a good adsorption on

electrode which is, however, less stable at extreme positive and negative potentials than the one used in this research.

Although the cause and effect are not well understood yet, this research group fortuitously found that pulsing the working electrode between the extreme potential limits in the presence of an organic solution saturated with carbon monoxide results an excellent surface coverage. The advantages of this method are that it provides a saturated and consistent surface coverage with a wider applicable potential window for the system. The detailed experimental procedures can be found in Table 2.2

2.5.3 Data Manipulation

Potential Difference IR Spectroscopy (PDIRS) was used to process all infrared data, single-beam infrared spectra were collected at a fixed electrode potential. Each single-beam infrared spectrum was ratioed with a second single-beam spectrum obtained either at an extreme potential at which the carbon monoxide had desorbed or at a potential that was 0.5 - 1V removed the sample potential. This potential difference method gave a consistent background independent of sample peak position. Peak frequencies calculated by Nicolet peak picking routine were then transferred to a spreadsheet program (Quattro Pro) for data analysis. Every experiment was repeated 3 - 8 times under the same conditions. Averaged peak frequencies of each electrode potential were used in linear regression to compute slopes and intercepts.

The differences of various conformations of tetra-*n*-alkyl groups and the size of cations were calculated by molecular modeling program (PCModel).

Table 2.2 Experimental Procedures†

1. Polishing the polycrystalline platinum working electrode with successively finer grades of suspended alumina (down to $0.05\ \mu\text{m}$) until mirror finish was obtained.
2. Removing embedded alumina from the electrode by immersing in an ultrasonic bath.
3. Assembling the working electrode with the spectroelectrochemical cell on mount.
4. Adding freshly prepared solution into cell (freshly distilled anhydrous solvent).
5. Deoxygenating the solution with dry nitrogen for 20 - 30 minutes.
6. Saturating the solution with CO by means of bubbling for 15 - 20 minutes.
7. Pulsing the working electrode between 2.0V and -2.0V versus SCE 5 times for 5 seconds at each potential.
8. Confirming the CO adsorption spectroscopically.
9. Purging the solution with dry nitrogen for 30 minutes to remove the remaining solution dissolved carbon monoxide.
10. Collecting data (128 scans at $2\ \text{cm}^{-1}$ resolution for each electrode potential).

† An electrochemical cleaning in acidic aqueous solution must be conducted in order to condition the electrode before changing the supporting electrolyte from one to another.

Chapter 3

Results and Discussion

3.1 Monolayer Surface Coverage

The first priority in data analysis was to verify monolayer surface coverage. Carbon monoxide adsorbed on platinum surface was first quantitated in acidic aqueous solution via the oxidization of CO to CO₂ by means of linear sweep voltammetry. The infrared peak area of the same adsorption collected prior to the linear sweep voltammetry was also obtained by integration. The charge required to oxidize carbon monoxide disclosed the surface concentration in acidic aqueous solution, to be $1.85 \times 10^{-9} \text{ M/cm}^2$, consistent with literature values [25 - 27]. Because there is no oxygen source in the acetonitrile used in this research (see experimental procedures), it is impossible to oxidize carbon monoxide in acetonitrile. To determine the surface coverage of carbon monoxide in acetonitrile is a little more complex. The ratio of surface concentration to peak area in aqueous solution must be calculated first. Peak areas from organic solutions were then correlated to this ratio. In addition to surface coverage calculated by correlation, both peak height (it obeys Beer's Law) and peak area indicated that pulsing the working electrode in a carbon monoxide saturated solution provided a saturated surface coverage which maintained monolayer and was consistent day by day.

3.2 Cyclic Voltammetry

Figure 3.1 is the cyclic voltammogram for adsorbed carbon monoxide on Pt electrode with 0.1M tetra-*n*-butylammonium perchlorate in anhydrous acetonitrile. It was shown on the cyclic voltammogram that there was no faradaic current between 2V and -1.8V versus SCE. The region of no faradaic current is called "double layer region". This means that no species were oxidized or reduced on electrode (the current present is due only to the charging of the double layer capacitance) and carbon monoxide was well adsorbed on electrode surface in double layer region. Test of monolayer coverage by IR was complementary and confirmed the result of the cyclic voltammogram. The double layer region available in acetonitrile solution should be compared with the potential range available in an acidic aqueous solution, approximately 500 mV. Changing the working electrode potential to a more positive value in aqueous solutions would oxidize carbon monoxide, and applying a more negative potential to the working electrode would end with the electrolysis of water. Organic solvents are obviously free of these limits until the more extreme potentials. The acetonitrile solutions provide a wider potential window for surface investigation without losing the surface coverage and without interfering faradaic processes. Acetonitrile has a potential window which is 8 times wider than that of aqueous solutions. Moreover, it absorbs much less infrared radiation than water so that the signal to noise ratio of carbon monoxide in organic solvent exceeds that for aqueous solutions. The S/N improvement due to

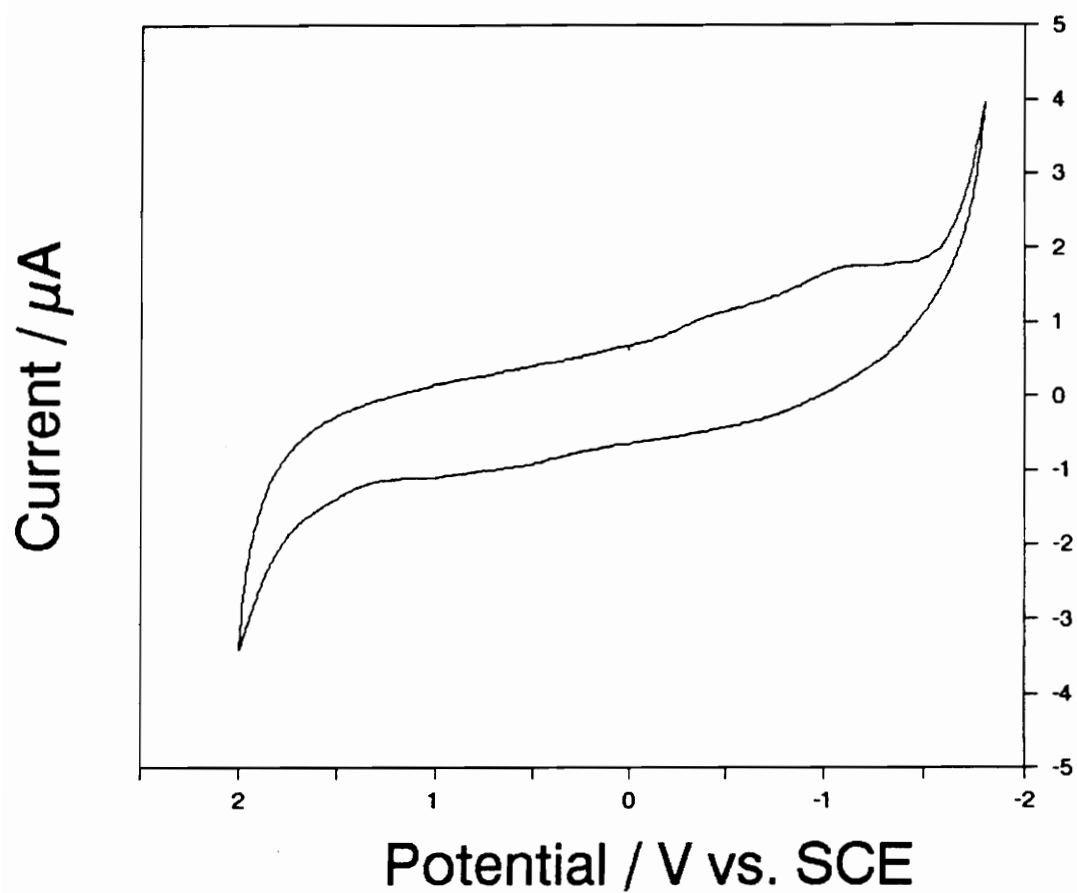


Figure 3.1 Cyclic Voltammogram of Adsorbed CO in Aqueous Solution obtained at a scan rate of 100mv/sec for an acetonitrile solution containing 0.1M tetra-*n*-butylammonium perchlorate electrolyte.

the smaller solvent absorption is beneficial because lower surface coverage may be more easily detected allowing studies of submonolayer coverage.

3.3 CO adsorbed on Platinum

Figure 3.2 shows the PDIRS spectra of carbon monoxide adsorbed on polycrystalline Pt working electrode with 4 different tetra-*n*-alkylammonium perchlorates as the supporting electrolytes. Figure 3.3 shows representative spectra of carbon monoxide in the presence of tetra-*n*-butylammonium perchlorate at different electrode potentials. All spectra collected in this research (about 2500 spectra) were almost visually identical except that the peak frequencies of carbon monoxide were potential and electrolyte dependent. Weaver et al. [24] observed when the electrode potential was shifted to extreme negative values, the peak frequencies of carbon monoxide shifted to lower position and then linear-bonded carbon monoxide was converted to bridged-bonded (peak occurred at approximately 1750 cm^{-1}). As shown in representative spectra, the peak positions of carbon monoxide in this research indeed shifted to lower frequencies if the electrode potential was changed to more negative values. However, in contrast to Weaver's experiment results, no evidence of site conversion was observed in all cases. Instead, carbon monoxide was ultimately desorbed and the peak height diminished at extreme negative potentials as well as extreme positive potentials. The result gave rise to a question: does pulsing the electrode between extreme potential limits give such a

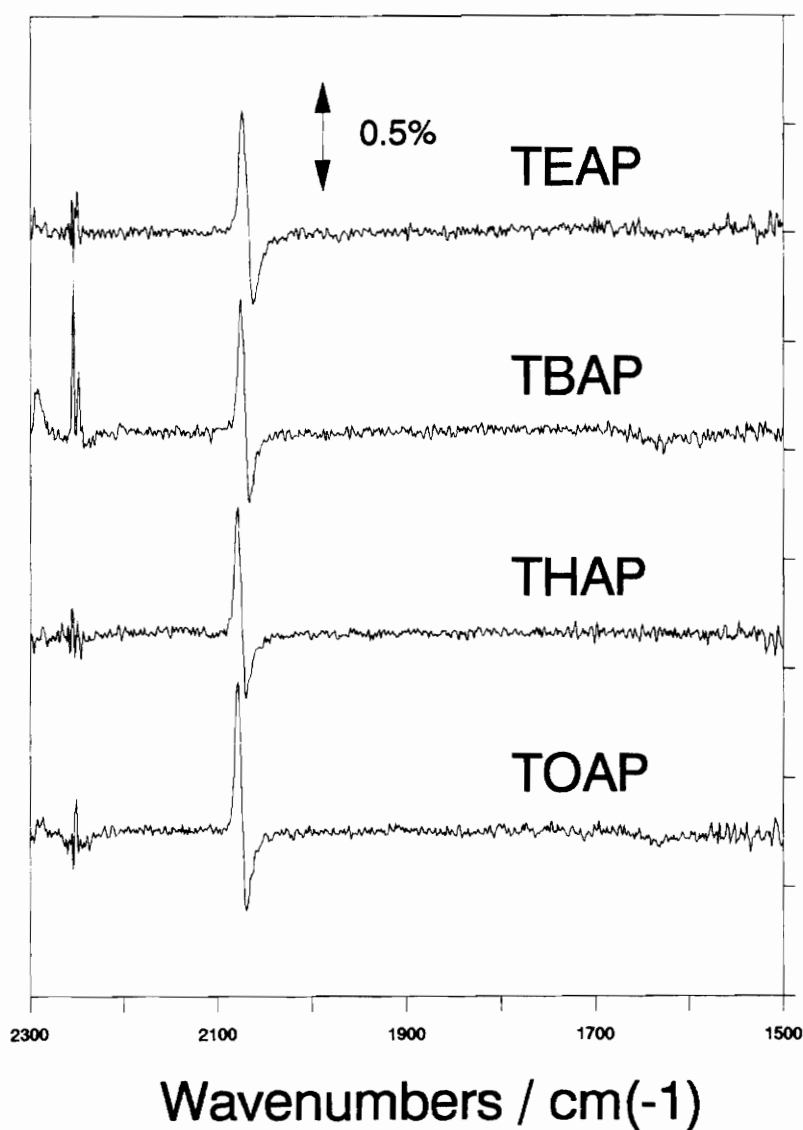


Figure 3.2 Spectra of CO Adsorbed on Pt in Tetra-*n*-alkylammonium Perchlorate/Acetonitrile. For each spectrum, the reference potential is 0.0V vs. SCE and the sample potential is -0.5V vs. SCE. The spectral features present at about 2250 cm⁻¹ are due to poor cancellation of the acetonitrile solvent bands in the different spectra.

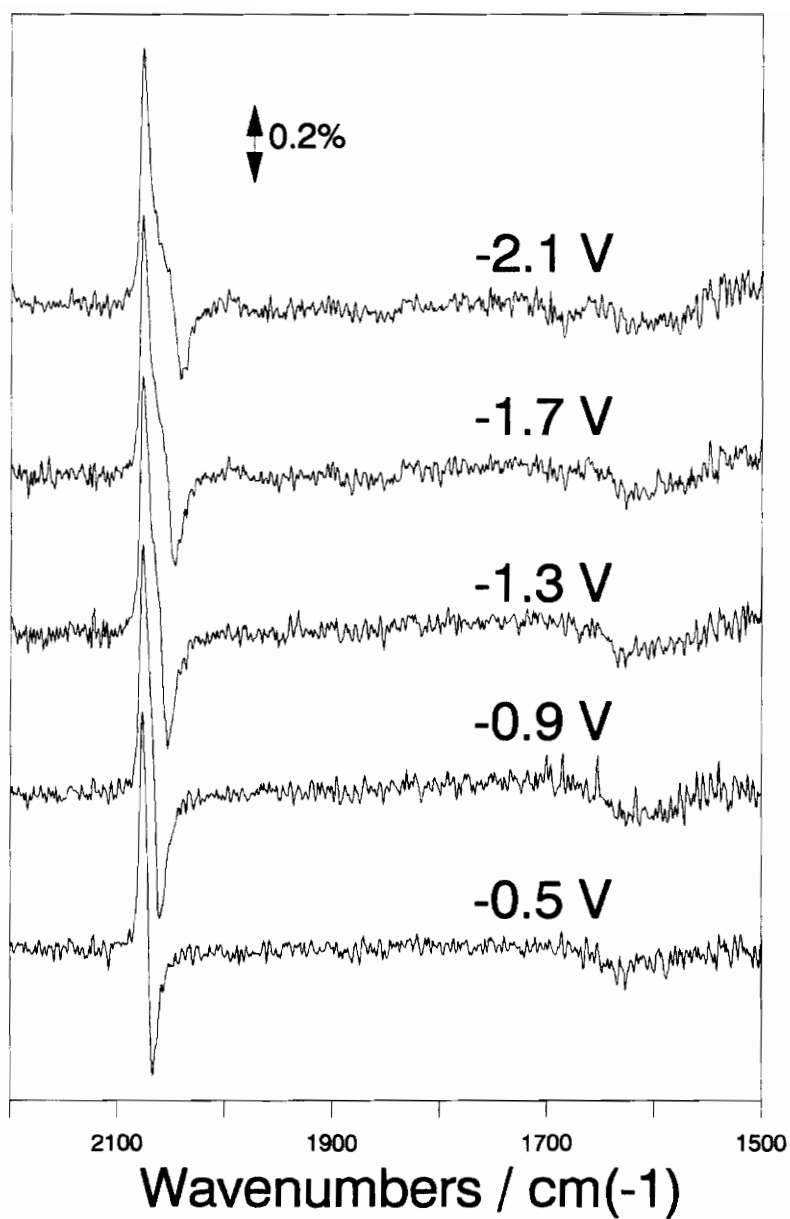


Figure 3.3 Representative Spectra of CO Adsorbed on Pt in TBAP/Acetonitrile. Each spectrum has 0.0V vs. SCE as the reference potential.

saturated surface coverage that there might not have enough unbonded platinum sites available on the electrode surface so that the site conversion was too low to be detectable? To investigate this argument, a series of experiments of unsaturated adsorption were conducted and compared with saturated adsorption.

3.4 Saturated versus Unsaturated Adsorption

Because carbon monoxide was desorbed at extreme potentials, plots of peak position versus electrode potential were not linear in the whole double layer region. Especially the data deviated from linearity on both two extreme ends. It could be corrected by checking the peak size of spectra, excluding those spectra of nonconstant surface coverage. Figures 3.4 - 3.7 are the plots of peak frequency versus electrode potential in the presence of 0.1M tetraethylammonium perchlorate (TEAP), tetra-*n*-butylammonium perchlorate (TBAP), tetra-*n*-hexylammonium perchlorate (THAP), and tetra-*n*-octyl perchlorate (TOAP) in anhydrous acetonitrile respectively. Owing to the fact of the low solubilities of tetramethylammonium perchlorate and tetra-*n*-decylammonium perchlorate in acetonitrile, 0.1M solutions of these electrolytes couldn't be prepared at room temperature, these two electrolytes were deleted from the list of investigation of the influence of cation size upon carbon monoxide infrared spectrum.

Table 3.1 is the slopes and related regression data of plots (Figures 3.4 - 3.7). Each peak frequency in Figures 3.4 - 3.7 was taken from the average of several

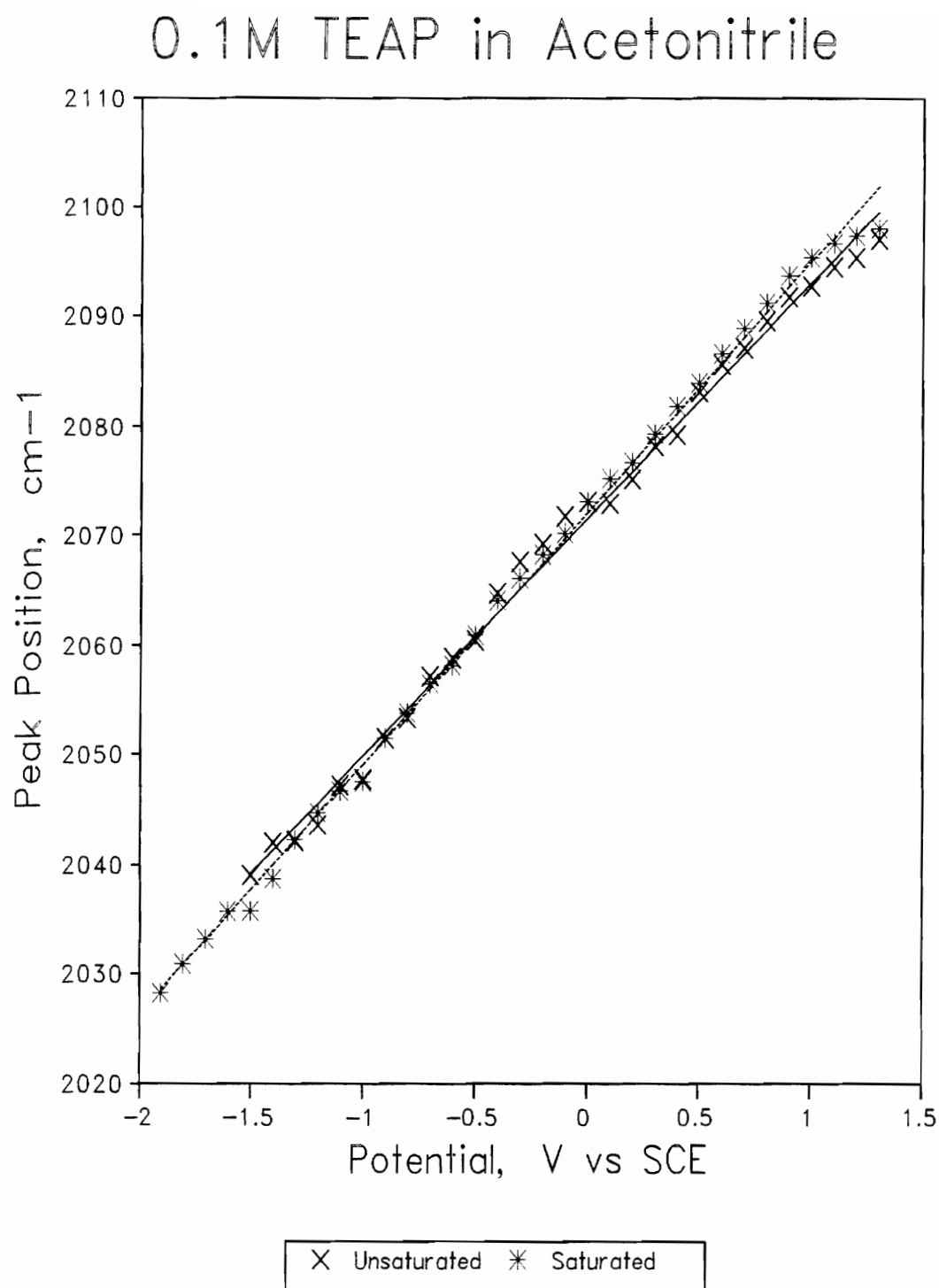


Figure 3.4 Plot of Peak Position versus Electrode Potential in the Presence of 0.1M TEAP in Acetonitrile

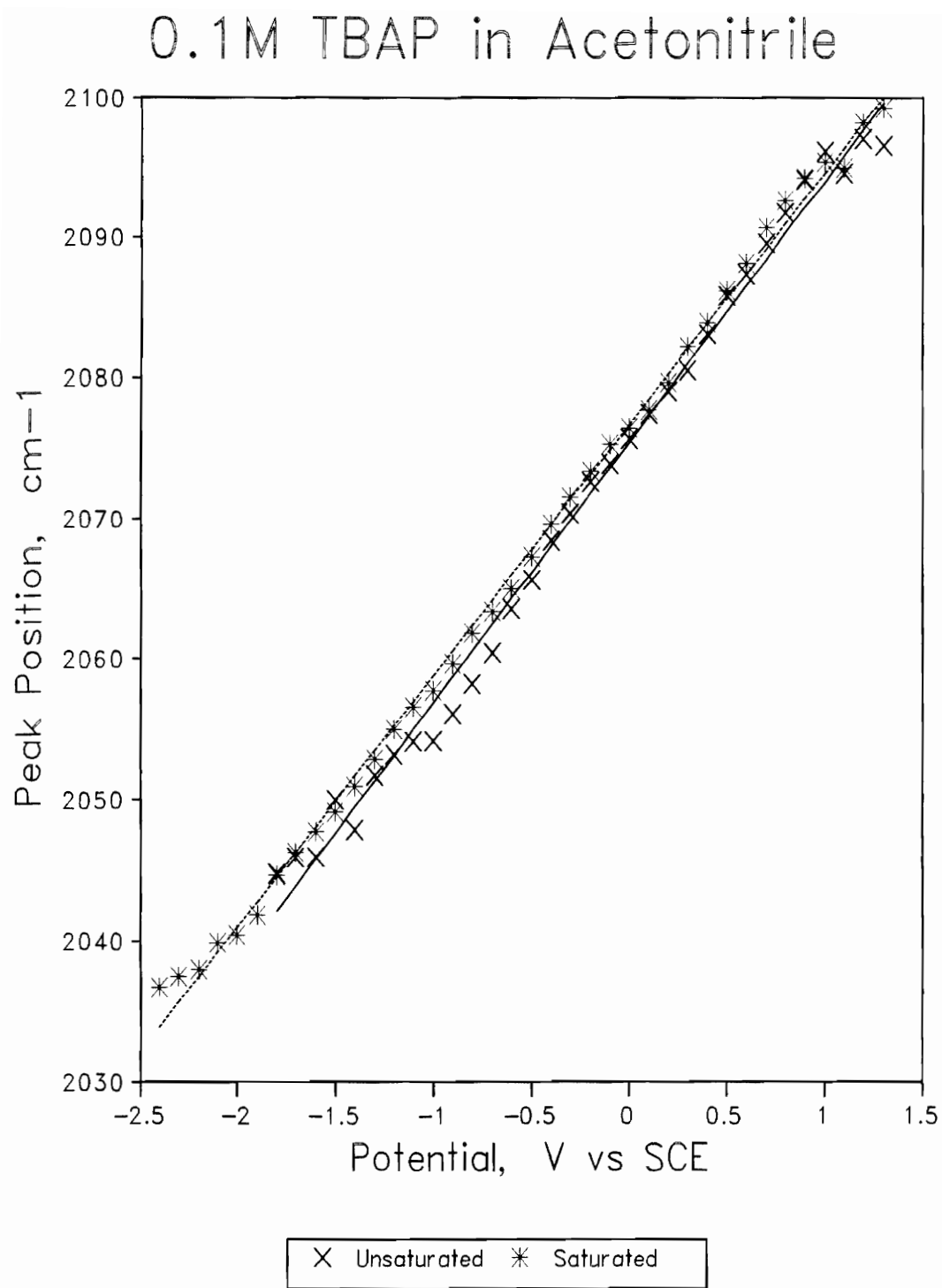


Figure 3.5 Plot of Peak Position versus Electrode Potential in the Presence of 0.1M TBAP in Acetonitrile

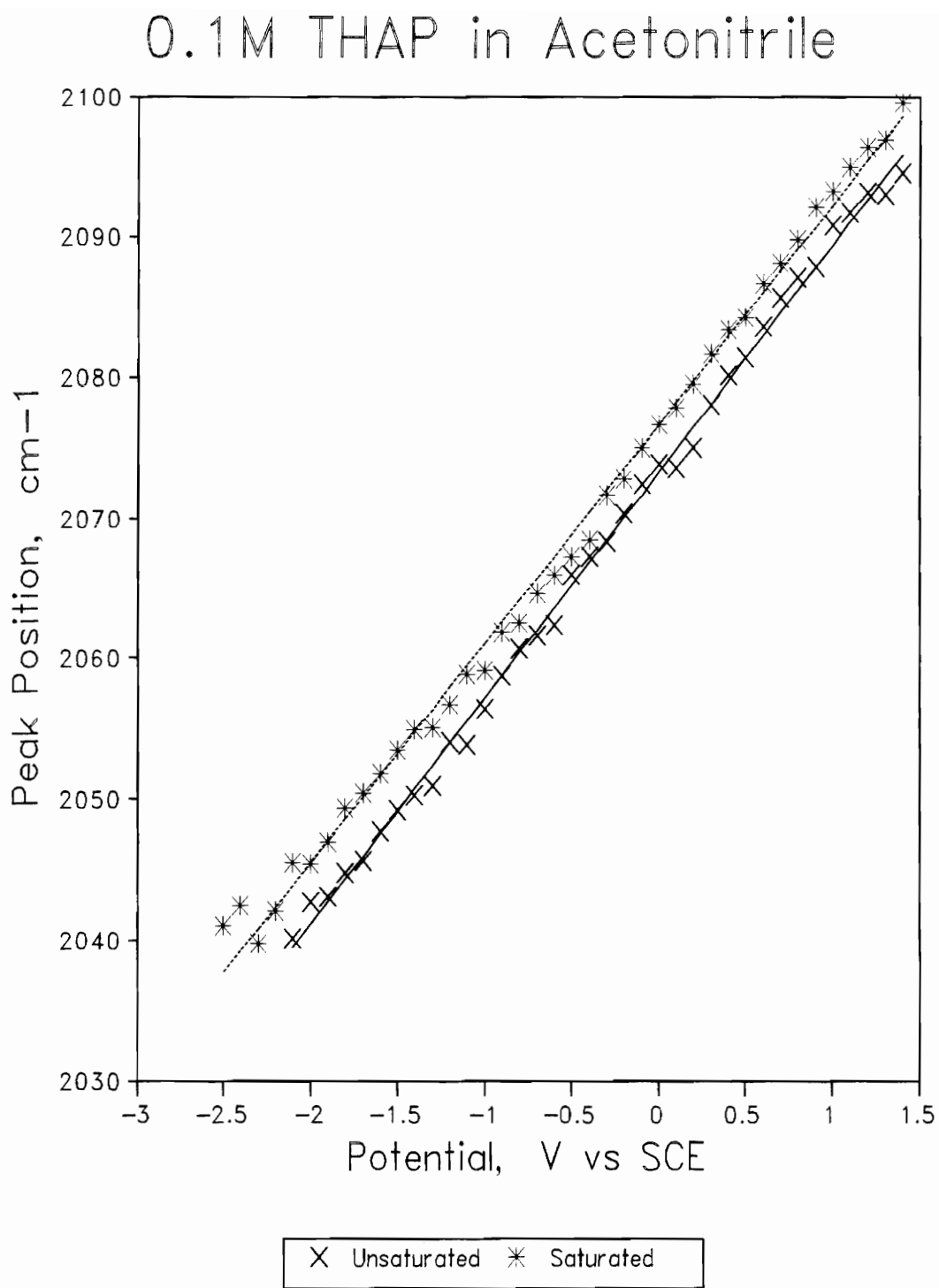


Figure 3.6 Plot of Peak Position versus Electrode Potential in the Presence of 0.1M THAP in Acetonitrile

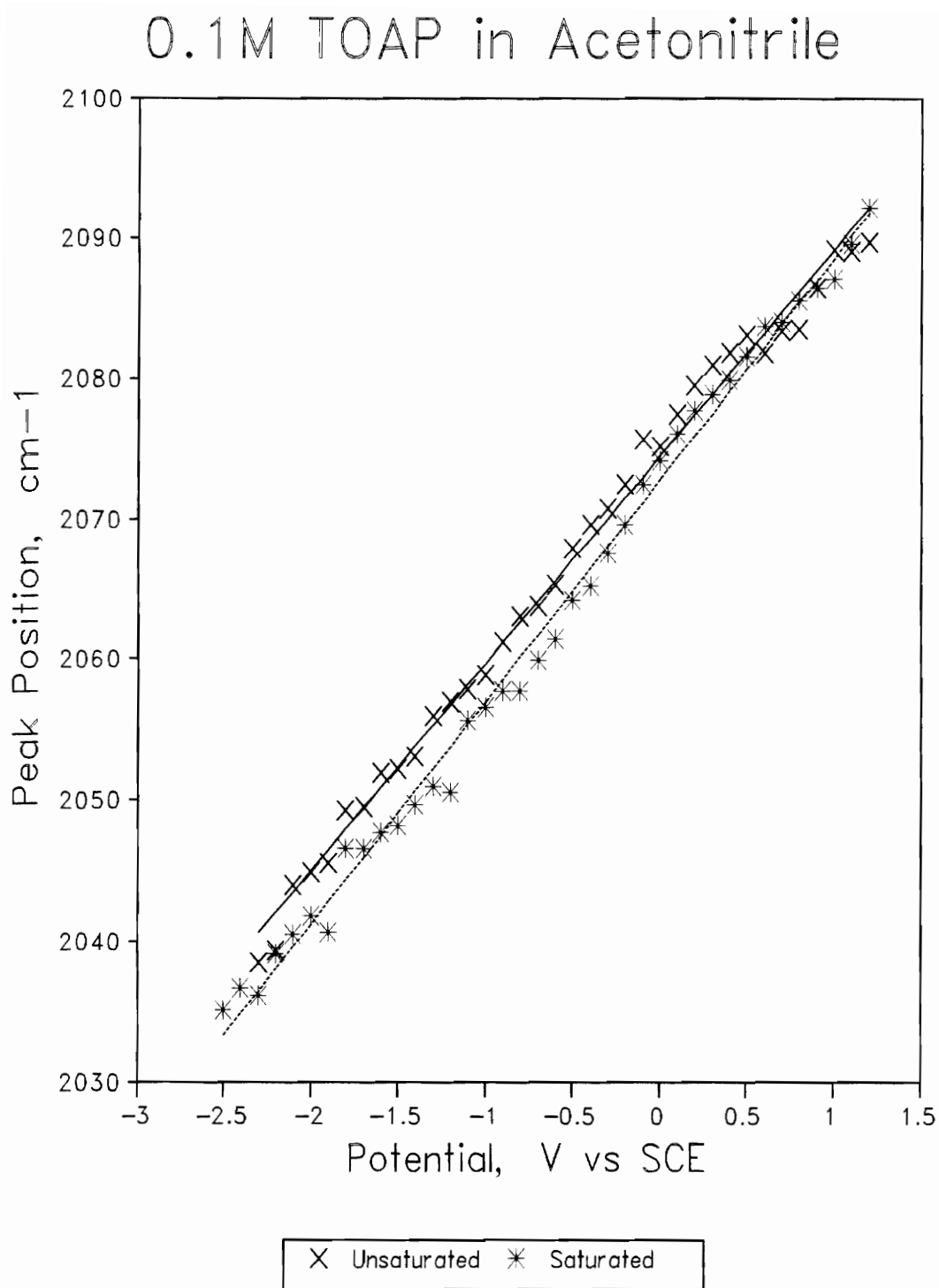


Figure 3.7 Plot of Peak Position versus Electrode Potential in the Presence of 0.1M TOAP in Acetonitrile

Table 3.1 Experiment Determined Stark Tuning Rates

Saturated Surface Coverage

	TEAP	TBAP	THAP	TOAP
Slope (cm^{-1}/V)	22.2	17.9	15.6	<u>15.8</u>
Standard Error of Slope	0.3	0.1	0.2	0.2
Intercept	2075	2076.7	2078	2078
Std Error of Intercept	1	0.9	1	1
Correlation Coefficient	0.995	0.998	0.996	0.994

Unsaturated Surface Coverage

	TEAP	TBAP	THAP	TOAP
Slope (cm^{-1}/V)	21.6	18.5	16.1	15.0
Standard Error of Slope	0.3	0.3	0.1	0.2
Intercept	2072	2075	2073.3	2074
Std Error of Intercept	1	2	0.9	1
Correlation Coefficient	0.994	0.992	0.998	0.993

independent experiments under the same experimental conditions. Linear regression was then performed on these averages with applied electrode potentials as the x parameters while corresponding averages of peak frequencies as the y parameters. It could be found in Table 3.1 that all correlation coefficients were greater than 0.992, indicating best fit straight lines and excellent linearity.

All plots in Figures 3.4 - 3.7 were linear and had excellent correlation coefficients, show that peak positions were dependent upon applied electrode potentials. This result agrees with the predictions of the Electrochemical Stark effect. On the other hand, under no condition were bridged bonded carbon monoxide observed in both saturated and unsaturated surface coverage. This makes the data coincide with Weaver's results in all aspects except the conversion from linear to bridged-bonded species, and is in contrast to the theoretical calculations of A. B. Anderson. Carefully analyzing Weaver's report, the following points were summarized: (1) Weaver did not observe the presence of bridged-bonded carbon monoxide in TBAP/acetonitrile solution, (2) the bridged-bonded carbon monoxide was found in sodium perchlorate/acetonitrile solution only. These points were in agreement with our results.

It seems that an extreme negative potential is not the only required experiment condition (ref. 2.1.3) for the conversion of carbon monoxide from linear-bonded to bridged-bonded. It is believed that the electrolyte cation has to have some interaction with both carbon monoxide and the electrode surface.

Coadsorption of alkali cation with carbon monoxide might further stabilize the bridged bonding in addition to the extreme negative potential [23]. Organic cations, apparently have either little or even no effect on stabilization of bridged bonding, suggesting that organic cations which can be easily expelled away from electrode surface by other more strongly interacting ions. Organic cations have either ultimately weak or virtually no interaction with both the adsorbed carbon monoxide and the electrode surface [39].

3.4.1 Effect of Surface Coverage on Stark Tuning Rate

The layout of Table 3.1 was arranged according to experiment conditions. The difference between columns was cation size and the difference between the upper and bottom halves was surface coverage. Thus, a comparison between the slopes of different electrolyte in the same row shows the influence of cation size. On the other hand, analyzing the effect of surface coverage should be done on the two slopes in the same column. All data in Table 3.1 were collected under virtually identical experiment conditions except cation sizes and surface coverage.

A comparison between saturated and unsaturated surface coverage was done mathematically by a statistical test. In the real world of measurement, reported data fluctuate around true values due to instrument precision and experiment uncertainty. Statistics can parse data pattern and distribution in order to tell how close two related values are. It is a measurement of reliability of experimental data. A

change in experiment parameter of Table 3.1 varied very little on slopes. It is very difficult to tell the difference among them without a systematic treatment. The advantages of applying statistical test to Table 3.1 are that it provides the probability of having the same true value for two numerically very close values and if the difference between them comes from uncertainty.

The pooled standard deviation of two slopes was first calculated by the following equations:

$$S_p = \sqrt{\frac{(n_1 - 1) S_1^2 + (n_2 - 1) S_2^2}{n_1 + n_2 - 2}} \quad (3.1)$$

$$v = n_1 + n_2 - 4 \quad (3.2)$$

where n_1 and n_2 are the numbers of observation, S_1 and S_2 represent the individual standard deviations of slope, and v is the degree of freedom.

A statistical t test was then performed using two-tailed t and 99% confidence interval with a t calculated by Equation 3.3:

$$t_{calc} = \frac{|b_1 - b_2|}{S_p} \quad (3.3)$$

where b_1 and b_2 are the slopes of two lines.

If t_{calc} is greater than the corresponding table value for the given degree of freedom, then the chance to have two different values is 99%.

Although the two slopes of each electrolyte in the same column in Table 3.1 looked very close, statistical treatment of the 4 pairs of slopes of saturated and unsaturated surface coverage for all four supporting electrolytes demonstrated that the slopes of the two unlike surface coverages are significantly different in statistics. The unsaturated surface coverage was obtained by reducing the quantity of carbon monoxide on electrode to one half of saturated surface coverage. Peak height of the unsaturated coverage was then verified spectroscopically to insure consistency from experiment to experiment. It has been shown by several research groups that the peak position is not only electrode potential dependent, but also surface coverage dependent [7, 40, 41]. This phenomena was not out of expectation, and actually in accordance with the deviation of peak position from linearity as the working electrode potential was shifted to extreme values at which peak size diminished and surface coverage reduced. Because peak position of carbon monoxide has some dependence upon surface coverage, it is not surprising to find that the rate of peak shift with applied electrode potential is also dependent upon surface coverage. Statistical tests gave the confidence to strongly support this conclusion.

3.5 Effect of Cation Size

Models of electrochemical double layer and Gouy-Chapman-Stern model both describes that the distance between outer Helmholtz plane and electrode surface has something to do with interfacial capacitance. In other words, the size of supporting

electrolyte cation plays a very important role in determining the properties of the electrode-solution interface where this distance is dominated by electrode cation size. The two models predict that the rate of peak shift is greater with smaller cation size at constant surface coverage. The slopes in Table 3.1 were verified with the theoretical prediction, all slopes followed the predicted trend, except TOAP, with saturated surface coverage. The slope for the saturated TOAP data is the only one out of eight which has a greater value with larger cation size rather than a smaller one. However, all other seven slopes show a regular decrease with increasing cation size, indicating there is a quantitative relationship between Stark tuning rate and cation size.

Table 3.2 gives the cation sizes calculated by molecular modeling program (PCModel), assuming spherical structures. Neglect the abnormal TOAP slope aside for later discussion. Plots of electrochemical Stark tuning rate versus reciprocal of cation radius provided that there is a linear relationship for Stark tuning rate and cation size (Figure 3.8). The correlation coefficients of plots in Figure 3.8 are 0.999 for unsaturated surface coverage and 0.993 for saturated surface coverage. This is a stunning and exciting result. So far in literature, theoretical predictions and experimental data only showed the trend. No quantitative relationship like this one has ever been determined. Therefore, some theoretical deductions are required to interpret this result.

Assuming that the capacitance corresponding to a parallel-plate capacitor

Table 3.2 Cation Sizes

	Radius, Å	Volume, Å ³	Surface Area, Å ²
TEAP	5.20	589	340
TBAP	6.62	1204	550
THAP	7.80	1988	764
TOAP (Extended)	8.57	2664	922
TOAP (Compact)*	<u>7.66</u>	1883	737

* Relative difference between extended THAP and compact TOAP

Volume	5.3%
Radius	1.8%

(Equation 2.1) is a good estimation for double layer capacitance. Let the outer Helmholtz plane (OHP) be an imaginary plate for the parallel-plate capacitor and the electrode surface is the second capacitor plate. The outer Helmholtz plane position, x_2 , is thus equal to the distance, d , between capacitor plates. Substituting Equation 2.1 into Equation 2.7 gives:

$$\delta_{vV} = \delta_{vE} \frac{A}{4\pi x_2} \quad (3.4)$$

Now the reciprocal of distance between the two capacitor "plates" is proportional to the electrochemical Stark tuning rate. If this is a correct prediction, then assuming that the imaginary plate surface area A remains constant in the whole double layer region, Equation 3.4 can be empirically written as:

$$\delta_{vV} = \frac{K}{r} + C \quad (3.5)$$

where C is a constant (regression intercept), r refers the cation radius, and

$$K = \delta_{vE} \frac{A}{4\pi} \quad (3.6)$$

It is not a surprise to have a nonzero intercept in Equation 3.5 because cation radius is less than the actual OHP position. The data in Tables 3.1 and 3.2 mathematically supported the relationship shown by electrochemical Stark effect, Equation 3.4. Furthermore, cation radius is also a good approximation for the distance from OHP to IHP. When the cation size approaches infinite, i.e., OHP is

effectively removed from system, the Stark tuning rate, δ_{vV} , is now equal to C , a nonzero part contributed by the potential drop from IHP to electrode metal surface. Because every electrochemical property in double layer originates from the potential drop across the double layer, and potential drops in series are additive, all quantities linearly related to potential drop are also additive. Therefore, δ_{vV} consists of two additive components:

$$\delta_{vV} = \delta_{IHP-OHP} + \delta_{IHP-Metal} \quad (3.7)$$

$$= \frac{k}{r} + \frac{k}{x_1} \quad (3.8)$$

where $\delta_{IHP-OHP}$ is contributed by the potential drop from IHP to OHP, $\delta_{IHP-Metal}$ is attributed to the potential drop from IHP to metal surface, and x_1 is the distance from IHP to electrode surface,.

It is obvious at this moment that the distance from IHP to metal surface can be obtained from Equation 3.8 (mathematically negative $1/r$ to make δ_{vV} zero). This method reveal an approximation of IHP position. Calculations demonstrated that for unsaturated surface coverage, IHP locates 17.49\AA above electrode surface and 44.99\AA for saturated surface coverage. OHP position then can be calculated by adding cation radius to IHP position:

$$x_2 = x_1 + r \quad (3.9)$$

where x_2 is the distance from OHP to electrode surface, x_1 is IHP position, and r

represents cation radius.

Table 3.3 gives the results calculated by Equation 3.9. Because the cation radii used are smaller than the actual solvated radii. The calculated values are greater than the true values. However, as shown in the table, IHP position is dependent upon surface coverage but kept constant in this research while OHP position varies with electrolyte cation radius. In brief, parallel-plate capacitor is indeed a good analogy for double layer capacitance and surface coverage specifically has some extent of influence on surface properties of electrode.

3.6 Molecular Modeling

Substitution of the abnormal TOAP slope in Table 3.1 into Equation 3.5 and plot of the point on the best-fit line in Figure 3.8 both exhibited that TOAP cation above the electrode saturated with carbon monoxide has the radius very close to THAP cation. Statistical t test again ascertained that all slopes with the same surface coverage are significantly different to each other except the slopes of THAP and TOAP of saturated surface coverage are the same statistically. The probability of having the same "true" value for either the two slopes or radii is 99% (Equations 3.1 - 3.3) even though the latter slope numerically looked greater than the former. For this reason, it is no doubt to conclude that TOAP cation changes size with surface coverage. The plot for saturated coverage in Figure 3.8 was used as a calibration curve to determine the "effective" radius of TOAP cation above the

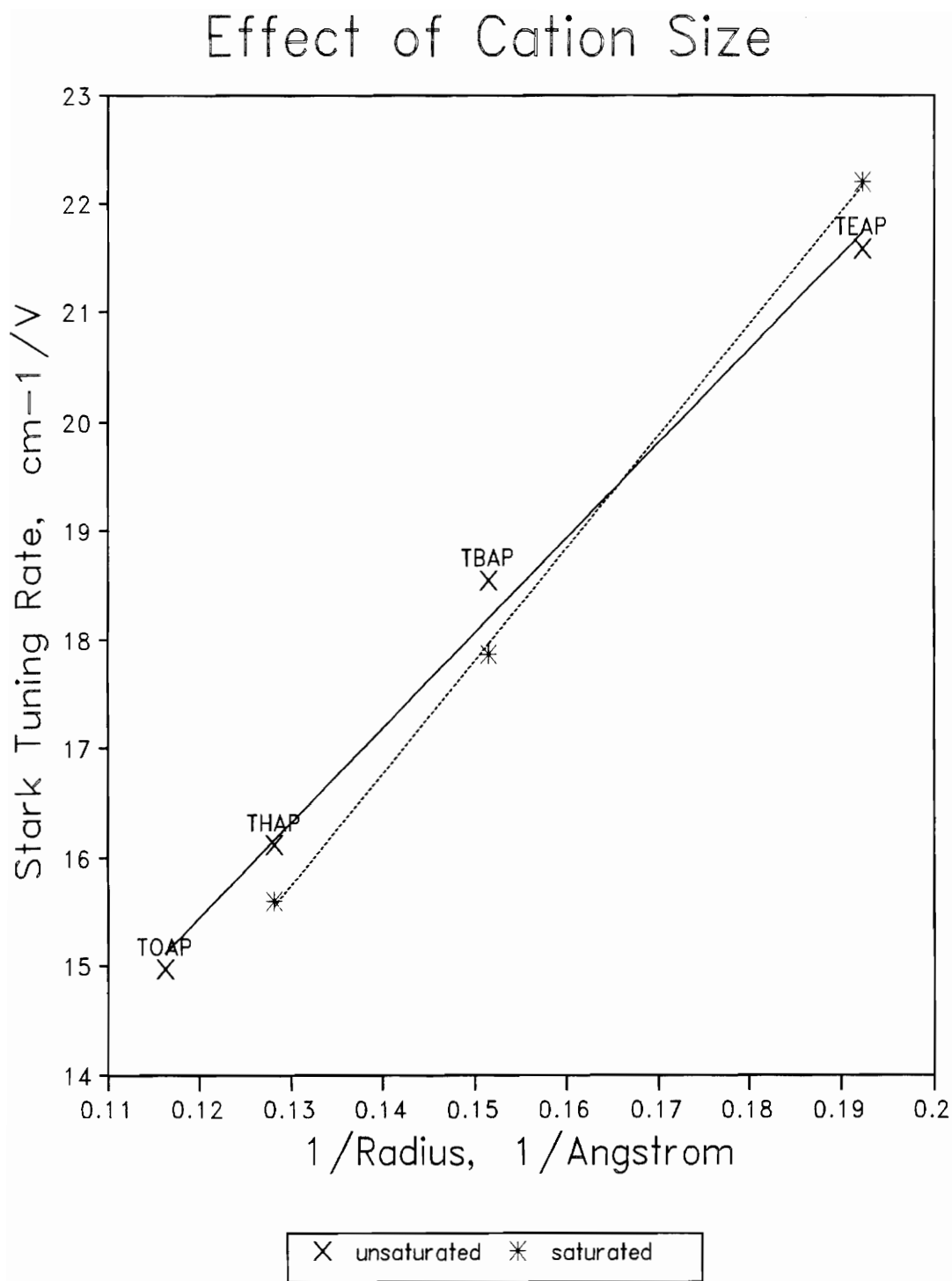


Figure 3.8 Effect of Cation Size upon Stark Tuning Rate

Table 3.3 IHP and OHP Positions

Saturated Surface Coverage

	IHP, Å	OHP, Å
TEAP	44.99	50.19
TBAP	44.99	51.59
THAP	44.99	52.79
TOAP (Compact)	44.99	53.09

Unsaturated Surface Coverage

	IHP, Å	OHP, Å
TEAP	17.49	22.69
TBAP	17.49	24.09
THAP	17.49	25.29
TOAP (Extended)	17.49	26.09

electrode saturated with carbon monoxide. The calculated radius for TOAP cation was found to be 7.66 ± 0.05 angstroms.

Molecular modeling program using MMX algorithm [42] was used to calculate various conformational sizes of TOAP cation (Table 3.2). Tetra-*n*-octylammonium cation, in a less soluble solvent environment such as acetonitrile, favors to be solvated in the more compact structure with the radius of 7.66\AA rather than the extended form with the radius of 8.57\AA . The radius of compact TOAP cation is well comparable with that of extended THAP cation (7.80\AA). The relative difference of the two radii is fairly small (1.8%, 0.14\AA) so that the instrument cannot distinguish the effect of such small radius variance due to its precision and experiment uncertainty. In contrast to saturated surface coverage, it was a totally different story for the TOAP slope with the electrode unsaturated with carbon monoxide, the slope followed the predicted trend and TOAP cation existed in extended form.

3.6.1 Effect of Surface Coverage on TOAP cation

TOAP is less soluble in acetonitrile than TBAP and THAP whereas TEAP is as soluble as TOAP. Although THAP has various conformational structures, it dissolves readily in acetonitrile, hence the solvent-THAP interaction helps the extended THAP cation to relax in solution without coiling itself into the more compact form. Additionally, the difference between the radii of extended THAP and compact TOAP cations is too small to be detectable. TEAP also senses the

same force exerted on TOAP in acetonitrile to change conformation because of its comparable solubility with TOAP. But TEAP cation is almost free of conformation. TOAP, on the other hand, possesses four long straight carbon chains and enough driving force from the surrounding (lower solubility), so TOAP cation generally stays in acetonitrile in its compact form. There must be some sort of mutual interaction to relieve the driving force of conformation when the electrode is unsaturated with carbon monoxide.

According to Fred C. Anson's investigation of ionic adsorption at electrode [39], the solvation energy of perchlorate anion in water is not great enough to prevent its adsorption on the surface of electrode. Moreover, perchlorate anion has a tendency to break up local solvent structure in water. This tendency gives perchlorate anion some hydrophobic character to facilitate its accumulation at the electrode-water interface. For the same reason, in an aprotic solvent such as acetonitrile, anions are less favorable than in water. Thus the "acetonitrilephobic" character of perchlorate anion is more notable than the hydrophobic character in water. The amount of accumulation at electrode should be greater in acetonitrile than in water.

It is easy to find that there are 9 pairs of lone-pair electrons on perchlorate anion besides the intrinsic -1 charge. An ion of such structure might have a sort of interaction with the electrode surface in addition to electrostatic force, perhaps being weakly adsorbed on the surface of Pt electrode by sharing a pair of electrons with

an empty Pt orbital. When the surface of Pt electrode is saturated by carbon monoxide, the adsorbed carbon monoxide covers all sites on electrode, acting like a film of coating or an insulator. The saturated coverage poisons and prevents the electrode from interacting with the counter ion, perchlorate anion and virtually no accumulation of perchlorate anion occurs. TOAP cations and perchlorate anions are surrounded by solvent molecules. The probability to have the two counter ions contact is nearly zero. TOAP cations in either double layer and bulk solution stay compact when the electrode surface is saturated with carbon monoxide. If the surface of electrode is not complete preoccupied, e.g. unsaturated with carbon monoxide, part of the platinum sites are exposed and available for perchlorate anions. The TOAP cations which formed OHP can approach the perchlorate ions accumulated on electrode surface. The induced interaction by opposite charges on the two counter ions stabilizes TOAP cations on OHP and breaks conformation barrier. However, because electrostatic force is a short-range force which is inversely proportional to the square distance between two charged particles, TOAP cations in bulk solution still remain compact and have virtually no effect upon surface properties and Stark tuning rate. Only cations locally bound above the electrode can extend themselves by means of counter ion interaction. Thus, it can be concluded that surface coverage is able to change conformational structure of TOAP on OHP.

Chapter 4

Summary

Electrochemical systems are complex to investigate and interpret. Many parameters are involved during the course of study. With precautions and careful designs, however, it has been proven in this work that several factors are able to influence peak position of carbon monoxide adsorbed on platinum.

The applied electrode potential has long been recognized as a major factor in the determination of peak position where there is a linear relationship between peak position and applied electrode potential. Solvent nature (aqueous versus organic), supporting electrolyte, and surface coverage are three other parameters that have been shown important in the influence of infrared peak position. The Stark tuning rates in acetonitrile varied from 22 to 14 cm^{-1}/V , dependent upon electrolyte cation size, which are less than the typical value of 30 cm^{-1}/V for aqueous solution. It was successfully demonstrated by experiment that the Stark tuning rate is inversely proportional to electrolyte cation radius. Electrochemical Stark effect predicts that the peak position is linearly dependent upon applied electrode potential. Models of the double layer and Gouy-Chapman-Stern model state the importance of distance from OHP to electrode surface. Integration of these three theories concludes the effect of electrolyte cation size upon Stark tuning rate. Experiment data are in agreement with all theoretical predictions. It has also been illustrated by this

research that the parallel-plate capacitor quantitatively describes well the double layer capacitance and coincides with the hypothesis of IHP and OHP. The Stark tuning rate of CO adsorbed on Pt electrode is inversely proportional to the cation radius.

Surface coverage modified electrode surface properties and changed the apparent IHP position above the electrode. IHP is pushed away from electrode surface if the electrode is saturated with carbon monoxide. The effect of surface coverage on Stark tuning rate is not as great as that of electrolyte cation size, although it can be proven by statistics that the change in Stark tuning rate with surface coverage is minor but significantly different. Surface coverage also relates to the degree of TOAP cation extension. It helps TOAP conformation only if the TOAP cations are locally bound above the electrode surface unsaturated with carbon monoxide because of short-range electrostatic force.

Bridged-bonded carbon monoxide was never observed in this research under all circumstance. Platinum crystal structure and coadsorption of alkali metal cation might be the two factors required for site conversion. No strong evidence is available so far to support this conclusion. It is worth aiming the study on this topic further.

Possible future developments could be the study of absorbed carbon monoxide behavior in the other organic solutions or different solvent compositions, using another probe molecule, and the investigation pulsing effect on adsorption.

References

1. J. K. Foley, C. Korzeniewski, J. Daschbach and S. Pons in A. J. Bard (Ed.), *Electroanalytical Chemistry*, Vol. 14, Wiley, New York, 1986, p309.
2. A. Bewick and S. Pons in R. E. Hester and R. Clark (Eds.), *Advances in Infrared and Raman Spectroscopy*, Vol. 12, Heyden, London, 1984, p1.
3. J. K. Foley and S. Pons, *Analytical Chemistry*, **56** (1985) 945A.
4. M. Fleismann, P. J. Hendra and A. J. McQuillan, *J. Chem. Soc. Chem. Comm.*, 80 (1973).
5. A. Bewick, K. Kunimatsu and S. B. Pons, *Electrochim. Acta.*, **25** (1980) 465.
6. A. Bewick and K. Kunimatsu, *Surf. Sci.*, **101** (1980) 131.
7. J. W. Russell, M. Severnson, K. Scanlon, J. Overend, and A. Bewick, *J. Phys. Chem.*, **87** (1983) 293.
8. D. K. Lambert, *J. Chem. Phys.*, **89** (1988) 3847.
9. D. K. Lambert, *Solid State Commun.*, **51** (1984) 297.
10. D. K. Lambert, *Phys. Rev. Lett.*, **50** (1983) 2106.
11. D. K. Lambert, *J. Vac. Sci. Technol. B*, **3** (1985) 1479.
12. K. Kunimatsu, W. G. Golden, H. Seki, and M. R. Philpott, *Langmuir*, **1** (1985) 245.
13. B. Beden, F. Hahn, S. Juanto, C. Lamy and J.-M. Leger, *J. Electroanal. Chem.*, **225** (1987) 215.
14. S. Juanto, B. Beden, F. Hahn, J.-M. Leger and C. Lamy, *J. Electroanal. Chem.*, **237** (1987) 119.
15. B. Beden, S. Juanto, J. M. Leger and C. Lamy, *J. Electroanal. Chem.*, **238** (1987) 323.

16. A. Papoutsis, J.-M. Leger and C. Lamy, *J. Electroanal. Chem.*, **234** (1987) 315.
17. M. R. Anderson, D. Blackwood, T. G. Richmond and S. Pons, *J. Electroanal. Chem.*, **256** (1988) 397.
18. A. E. Russell, S. Pons and M. R. Anderson, *Chem. Phys.*, **141** (1990) 41.
19. J. G. Love and A. J. McQuillan, *J. Electroanal. Chem.*, **274** (1989) 263.
20. K. Ashley, M. G. Samant, H. Seki and M. R. Philpott, *J. Electroanal. Chem.*, **270** (1989) 349.
21. A. B. Anderson, *J. Electroanal. Chem.*, **280** (1990) 37.
22. S. P. Mehandru and A. B. Anderson, *J. Phys. Chem.*, **93** (1989) 2044.
23. E. L. Garfunkel, J. E. Crowell and G. A. Somorjai, *J. Phys. Chem.*, **86** (1982) 310.
24. J. D. Roth, S.-C. Chang and M. J. Weaver, *J. Electroanal. Chem.*, **288** (1990) 285.
25. L.-W. H. Leung and M. J. Weaver, *J. Phys. Chem.*, **241** (1988) 4019.
26. D. S. Corrigan and M. J. Weaver, *J. Electroanal. Chem.*, **241** (1988) 143.
27. L.-W. H. Leung and M. J. Weaver, *J. Electroanal. Chem.*, **272** (1989) 161.
28. F. A. Cotton and G. Wilkinson, *Advanced Inorganic Chemistry*, 5th Ed., Wiley, New York, 1988, p59.
29. B. Douglas, D. H. McDaniel, and J. J. Alexander, *Concepts and Models of Inorganic Chemistry*, 2nd Ed., Wiley, New York, 1983, p48.
30. A. J. Bard and L. R. Faulkner, *Electroanalytical Methods*, Wiley, New York, 1980, p9.
31. *CRC Handbook of Chemistry and Physics*, 67th Ed. CRC Press, Boca Raton, 1986, p.F-71
32. A. J. Bard and L. R. Faulkner, *Electroanalytical Methods*, Wiley, New York, 1980, Ch. 12.

33. A. Bewick and S. Pons in R. E. Hester and R. Clark (Eds.), *Advances in Infrared and Raman Spectroscopy*, Vol. 12, Heyden, London, 1984, p5.
34. J. K. Foley, C. Korzeniewski, J. Daschbach and S. Pons in A. J. Bard (Ed.), *Electroanalytical Chemistry*, Vol. 14, Wiley, New York, 1986, p314.
35. A. J. Bard and L. R. Faulkner, *Electroanalytical Methods*, Wiley, New York, 1980, p585.
36. J. K. Foley, C. korzeniewski, J. Daschbach, and S. Pons in A. J. Bard (Ed.), *Electroanalytical Chemistry*, Vol. 14, Wiley, New York, 1986, p316.
37. J. K. Foley, C. korzeniewski, J. Daschbach, and S. Pons in A. J. Bard (Ed.), *Electroanalytical Chemistry*, Vol. 14, Wiley, New York, 1986, p323.
38. H. O. House, E. Feng and N. P. Peet, *J. Org. Chem.*, **36** (1971) 2371.
39. F. C. Anson, *Acc. Chem. Res.*, **8** (1975) 400.
40. R. M. Hammaker, S. A. Francis and R. P. Eischens, *Spectrochim. Acta*, **21** (1965) 1295.
41. A. Crossley and D. A. King, *Surf. Sci.*, **68** (1977) 528.
42. J. J. Gajewski, K. E. Gilbert and J. McKelvey in E. Liotta (Ed.), *Advances in Molecular Modeling*, Vol. 2, JAI Press, Greenwich, 1990, p.65.

Vita

Jimin Huang was born on September 30, 1961 in Taipei, Taiwan, the Republic of China. He received his Bachelor's degree in chemistry from Chinese Culture University, Taipei, Taiwan in June 1984. After finishing two years of compulsive military service in Chinese Artillery, The National Science Council of Taiwan hired him as a research technician in organic synthesis. He held that position until his enrollment at Virginia Tech in August 1989 where he changed the area of interest and devoted himself to analytical chemistry study under the guidance of Professor Mark R. Anderson.

黃之銘 Jimin Huang